Universidade do Minho

Escola de Engenharia

Pedro Cancela Gomes

Degradation Behaviour and Reuse of Selective Laser Sintering PA12 Powders

Dissertação de Mestrado

Mestrado Integrado em Engenharia de Materiais

Trabalho realizado sob a orientação de

Professora Doutora Olga Machado Sousa Carneiro

E

De

Professora Doutora Alexandra Manuela Vieira Cruz Pinto

DECLARAÇÃO DE INTEGRIDADE

Declaro ter atuado com integridade na elaboração do presente trabalho académico e confirmo que não recorri à prática de plágio nem a qualquer forma de utilização indevida ou falsificação de informações ou resultados em nenhuma das etapas conducente à sua elaboração.

Mais declaro que conheço e que respeitei o Código de Conduta Ética da Universidade do Minho.

Agradecimentos

Esta dissertação, marca, não só o fim do meu ciclo de estudos, mas também de uma das fases mais importantes da minha vida. Durante estes 5 anos de universidade, muitas foram as pessoas que contribuíram e tornaram esta, uma etapa que nuca irei esquecer.

Em primeiro lugar, faço chegar um agradecimento especial aos meus pais, sem o seu apoio, sacrifício e confiança, nada do que concretizei até agora seria possível. Obrigado por tudo o que fizeram por mim.

Às minhas orientadoras, Olga Carneiro e Alexandra Alves, um obrigado por todas as dicas, por toda a ajuda e por toda a paciência que demonstraram comigo durante toda a realização desta dissertação. Todos os seus conhecimentos foram fulcrais para a construção da mesma.

A todos os colegas que me acolheram e ajudaram na empresa, o meu obrigado. Em especial, ao Nuno Costa pela oportunidade que me deu e ao Oscar Piñeiro por toda a ajuda e orientação. Ao Mário, agradeço toda a paciência na realização da análise das amostras em CT.

Um obrigado enorme à minha namorada, a pessoa que me acompanhou em todos os passos e decisões que tomei desde que nos conhecemos. Obrigado por me aturares, mesmo quando é difícil fazê-lo, e estrares sempre ao meu lado quando preciso.

Um obrigado gigante aos meus amigos, aqueles que sempre me apoiavam durante os tempos mais difíceis e que todos os dias me faziam rir a toda a hora. Foi a universidade que nos uniu e sem vocês estes últimos 5 anos não seriam tão especulares como foram. Sem dúvida os melhores da minha vida que jamais esquecerei.

Por último, obrigado à minha família, todo o vosso apoio e motivação ajudaram a que todo este percurso se realizasse do início ao fim. Obrigado por nunca duvidarem de mim.

Resumo

A Sinterização Seletiva a Laser (SLS), é uma tecnologia da família da manufatura aditiva, um ramo da engenharia que se dedica à produção de peças prontas ao uso através da construção/impressão das mesmas camada-a-camada, usando a matéria-prima em forma de pó. Esta técnica, destina-se sobretudo à impressão de materiais poliméricos, entre eles a poliamida 12 (PA12), permitindo uma grande liberdade de geometrias e boa qualidade das peças impressas, seja ela visual ou em termos de propriedades mecânicas.

Após o fabrico por esta tecnologia, uma quantidade significativa de pó não é sinterizada, sendo então recolhido para reaproveitamento. No entanto existem fenómenos de degradação, especialmente térmica, limitando a sua reutilização, sendo que os fornecedores geralmente aconselham a que o número de reutilizações não ultrapasse as 12 e sempre com uma mistura de 50% de material virgem.

Estes fenómenos de degradação foram estudados, através de ensaios de caracterização mecânica (testes de tração uniaxial), caracterização térmica por DSC, caracterização visual através de observação do estado das peças impressas e visualização do pó ao SEM e caracterização da porosidade por tomografia computorizada (CT). Com estes, foi concluído que, uma degradação do pó é evidente, especialmente do ponto de vista visual, afetando as características da peça impressa e comprometendo o seu correto funcionamento. O fator mais relevante notado, foi o aumento da porosidade interna das peças impressas, que para os ciclos mais avançados testados foi de tal maneira elevado que levou ao colapso das paredes da peça para o seu interior.

No entanto, devido ao facto de esta tecnologia possuir um método de reciclagem bastante seletivo, os efeitos da degradação são atenuados, nomeadamente no que toca ao desempenho mecânico, que não piorou significativamente para os ciclos testados.

Concluiu-se então, que a degradação do pó reutilizado em impressões por SLS tem de ser tido em conta e compreendido, mas esta tecnologia em si, mesmo quando utiliza matéria-prima virgem ou pouco reutilizada, já apresenta dificuldades em reproduzir resultados repetitivos.

Abstract

Selective Laser Sintering (SLS) is an additive manufacturing technology dedicated to the production of parts through a layer-by-layer printing process, using a building material in the form of powders. This technique is intended mainly for the printing of polymeric materials, such as polyamide 12 (PA12), enabling enormous geometrical freedom and good quality of printed parts, either in terms of visual aspect, or mechanical properties.

In SLS, after the manufacturing process, a large quantity of the powders is not sintered, which is recovered for reuse. However, degradation phenomena are present in this unsintered powder, namely thermal degradation, which limits its reuse. Thus, the suppliers advise a maximum of 12 cycles of reuse and always with a ratio of 50% virgin material.

These phenomena were studied through a series of characterization techniques, mechanical analysis (uniaxial tensile tests), thermal characterization by DSC, visual characterization of printed parts, visualization of the powders by SEM, and porosity characterization by computed tomography (CT). With these, it was concluded that it is evident both visually and performance-wise. The most relevant factor noted, was the increase in internal the porosity of the printed parts, which for the most advanced cycles tested was so extreme that forced the printed part´s walls to collapse on each other.

However, due to this technology having a very selective recycling process, the effects of degradation are minimized, namely when mechanical behaviour is concerned, which did not worsen significantly for the cycles tested.

It was concluded that degradation of the reused powder used in SLS printing, has to be considered and comprehended, but this technology, even when new or semi-new powder is used, already presents reproducibility and repetitiveness problems.

TABLE OF CONTENTS

List of figures

List of tables

List of abbreviations

A

AM – Addictive Manufacturing

B

BSE – Backscattered electrons

C

CAD – Computer-aided design

CT – Computed tomography

D

DSC – Differential Scanning Calorimetry

E

EDS – Energy-dispersive X-ray spectroscopy

F

FFF – Fused filament fabrication

M

MFR – Melt Flow Rate

P

PA12 – Polyamide 12

R

RP – Rapid prototyping

S

SE – Secondary electrons

SEM – Scanning Electron Microscopy

SLA – Stereolithography

SLS – Selective Laser Sintering

STL – Standard triangle language

T

$T_{m,\ peak}$ – Melting temperature

TP – Test pieces

U

UV – ultra-violet

Numbers

3D – Three-dimensional

CHAPTER 1 – INTRODUCTION

1. Introduction

This chapter presents a brief motivation of this work and a presentation of *NM3D Ibérica, Sistemas de Metrologia Industrial*, the company, where this work was developed. An outline of the different chapters of this dissertation is also presented.

1.1. Motivation

Additive manufacturing (AM) technologies have been gaining prominence in the industrial world. One technology belonging to this particular family of technologies is the Selective Laser Sintering (SLS) process. SLS is increasingly chosen as a way to manufacture functional parts, with great dimensional precision, a wide variety of materials, and a relatively low processing time, for different application areas, like automotive, aerospace, medical, among many others [1], [2].

This technology is becoming a popular choice for applications either requiring rapid prototyping (RP) or even large-scale manufacture requiring a large degree of customization. With the development of new and cheaper ways to use this type of technology, more and more companies are able to use a technology previously limited to high-tech industries [3].

Contrarily to traditional subtractive technologies, the use of SLS, and AM techniques in general, brings some advantages, such as no need for mould tooling, removing constraints normally associated with the traditional methods of subtractive manufacture [4].

Although a good choice, SLS has one major problem to be solved. The large percentage of the powders used in the powder bed is not sintered, causing a great potential waste that has negative economic and environmental impacts. Thus, a common strategy used to minimize these impacts is to reuse the powders. However, the high temperatures (around 180 °C in the case of PA12 powders) on the printing equipment chamber and long residence times (a minimum of 3 hours in the equipment used) may lead to changes on the properties of the powders, limiting its number of recycling cycles and incorporation rate [5]. Because of that, the unused powders are recycled and reprocessed. However, the powders need to be carefully treated to allow their reuse, although it may still compromise the quality of the printed part [6]. Understanding the behaviour of these powders after each recycling cycle is of extreme importance. A more detailed view of how the recycling process works in SLS processing is explained later in this document.

1.2. Company presentation

This thesis was developed in *NM3D Ibérica, Sistemas de Metrologia Industrial* company. This company, with headquarters based in Vila Nova de Cerveira, started its activity with the commercialization of metrology equipment and the render of metrology-related services, offering a variety of personalized solutions for a vast field of operation. With a young team of collaborators and the focus on continuous improvement of their services, the company has grown to be an important mark in this field. Through the years and, intending to stay on the vanguard of technology, *NM3D Ibérica* decided to enter in the additive manufacturing world, recognizing the relevance that this type of technology will have in the near future. Since then, *NM3D Ibérica* acquired a variety of AM technology equipments and started to sell services in this area, always following the philosophy of continuous improvement that characterizes the company.

1.3. Structure of the thesis

Chapter 1 – Introduction and motivation, presentation of *NM3D Ibérica*, and thesis outline.

Chapter 2 – State of the art. A summary of the AM technologies, with emphasis on SLS technology is given. The advantages and the limitations of SLS are described.

Chapter 3 – This chapter describes the material and methods used in the fabrication and characterization of both powders and processed samples.

Chapter 4 – This chapter presents the results and their discussion.

Chapter 5 – The main conclusions of the thesis and considerations for future works are presented in this chapter.

CHAPTER 2 – STATE OF ART

2. State of the art

This chapter aims to provide knowledge about the technology, materials, and characterization techniques that will be a part of the making of this thesis.

2.1. History of additive manufacturing

Initially created to produce prototypes rapidly, only for visual purposes, for example in design approval or fit-to-form tests, and later evolving to the production of parts with properties similar to the same product produced with classic techniques, although less functional mechanical-wise depending on the desired use, AM is a fabrication field in constant evolution. Nowadays, AM can be used to create functional parts in the industrial field, reaching geometries impossible to achieve with any other type of manufacturing technology [6], [7].

Considered by many to be a part of the fourth industrial revolution (industry 4.0), and commonly associated with other technologies such as robotics and digitalization, it is important to understand how and why this family of technologies is changing the way industries are approaching the processing of complex but functional parts for the vastest areas of use. More commonly known as 3D-printing or RP, the term additive manufacturing refers to any technology, based on the production of parts layer-by-layer from a computer-aided design (CAD) 3D model, previously constructed [1], [8], [9]. Dating back to the '80s, the first commercially used AM technology consisted of the use of a UV source to harden a UV-sensitive polymer (photo-polymer) building the desired structure, thus being the first SLA equipment in this field. Even though it was innovative, this technology was also very expensive and not reliable [10]–[12].

2.2. The concept of SLS technology

As already mentioned, the premise of this type of technology is to produce the parts layer-by-layer, allowing the development of extremely complex shapes. Among all the technologies in the AM family, SLS stands out as an interesting technique that is based on the sintering of selected zones of a powder bed, of the chosen material, through a laser beam (the most common type are CO_2 lasers, although there are other types like diode lasers) usually in an oxygen-free building chamber. The solid part is made layer-by-layer, where the feed cartages ascend (through electric pistons) one at a time in alternate layers, supplying the desired quantity of powder. Then a recoater (in the form of a roller or blades) spreads the powder, covering the building table (which descends when the feed cartridges ascend). Lastly, through a conversion software, an STL file is transformed into code lines that will guide the CO_2 laser to only focus on the desired powder grains, not affecting

the surrounding ones, breaking their surface tension, and sintering them together, creating (sintering) a solid part. This process is achieved because the chamber where the sintering occurs is previously heated to a temperate just below the melting point of the material, being the energy supplied by the laser sufficient to melt the powder grains. This chamber heating and subsequent slow cooling also helps to minimize part warping and distortions. The accuracy of SLS machines is dependent mainly on the used material, with new and more dimensional accurate powders being developed every day [6], [13]–[15]. Figure 1 shows the usual setup of an SLS machine.

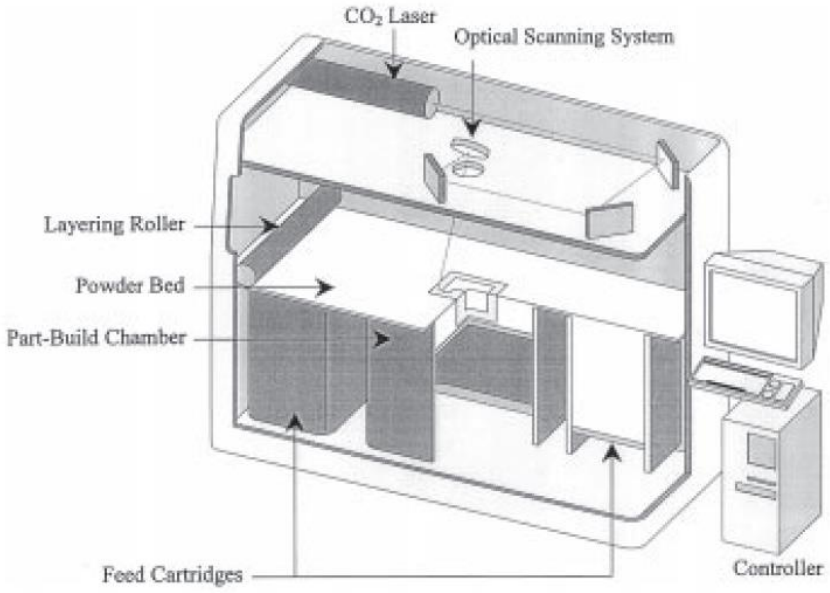

Figure 1 - Equipment setup from a SLS machine, from [4].

This type of technology has been featured in the additive manufacturing world due to its advantages, not only when compared with traditional techniques but also with the other AM techniques. Concerning the advantages, it has over the traditional processes, SLS shows the freedom for complexity of geometry and the capability of easy customization. There is some limitations regarding the different types of materials available for this technology, being the polyamide powders those who dominate the market, and the unprocessed portion of the powder bed used can be recycled. Lastly, the printing speed, the easiness of process control, higher dimensional accuracy (when compared with FFF), and the capability to self-sustain the structures it builds, removing the need for support structures like the ones present in fused filament fabrication 3D printing makes the SLS stand out as an excellent productive option. The elimination of supporting structures offers certain advantages, like the possibility to have a dense spatial distribution of parts, and reducing the post-processing tasks, saving time, and increasing

productivity [16], [17]. As mentioned previously, there is a long list of materials used in SLS, which includes polymers, metals, and ceramics (the technology slightly changes depending on the material). However, polymers are the main elements of this list [18].

Although all the advantages that SLS brings to the AM scene, it still has some limitations and problems to be solved. One of the most critical limitations is the fact that 80-90% of the material in the chamber is not sintered. However, due to the high temperatures that it is subjected to during the printing process, alterations on its properties are induced, complicating its reuse. An example of this phenomenon can be the agglomeration of the powders, which reduces their flowability, making it hard to build a homogeneous powder bed. Also, a decrease in the physical and mechanical properties of the material can occur, compromising the quality of the produced parts [14], [18].

2.3. SLS process and PA12 powders

Amongst the SLS technologies, polymeric materials are undoubtedly the most used, being the Polyamides or their blends about 95% of the materials commercially sold. PA12 is the most common one, for its easy and flexible SLS processing (see Figure 2). This is due to the fact that PA12 has a large interval between the start of melting during the heating process and the start of crystallization in the cooling process, which allows keeping the material heated without crystallization until the cooling stage, maximizing consolidation and preventing warpage [18], [19].

PA12 is a semi-crystalline polymer where the monomers are linked by amide groups, and some of them may contain open-end chains, which may be susceptible to post-condensation and crosslinking reactions when subjected to higher temperatures, as is the case of the SLS process, altering the processing response of the polymer. Some of the properties that make it the most used polymer in the SLS process include not only its mechanical properties but also low moisture

Figure 2 - Examples of PA12 printed parts by SLS

absorption, when compared with other polyamides, remaining stable in humid environments, good resistance to abrasion, and good resistance to chemicals including solvents [19],[20].

2.4. Powder degradation in the SLS process

In the SLS process, there are two main types of "powders waste": the powders that remain in the building table, unsintered, called partcake material, and the excess powders used for the bed that directly falls into the feeders, called feed material (see Figure 1). The partcake material is the one that suffers the most severe thermal effects once it remains at high temperatures longer than the feed material. Thus, the "aging" of the powders, depends mainly on the building temperature of the chamber and residence time, where the severity of powders degradation increases with the increasing of both parameters. Specifically, studies showed that the predominant degradation processes that occur in polyamides are the cross-linking and chains scission [12].

The reuse of unsintered powders is a relevant economic and environmental issue. One of the ways to reduce the negative effects of powders degradation is the incorporation of flow and antistatic agents, to increase their flowability. These antistatic agents have a very small size (around 1 μm) and are added in small quantities, between 0.05-1.5 wt %. Their effect is to eliminate the static charge present in the powders, reducing their tendency to agglomerate and improving flowability. Nevertheless, this flow and antistatic agents may negatively affect the mechanical integrity of the printed parts, a disadvantage that must be considered [16].

On the other hand, low-temperature SLS can also be used to minimize powders degradation. As the name suggests, this technique is based on the maintenance of the powder and the powders bed at lower temperatures, reducing the degradation of the material. Although this might sound simple, it increases the chance of curling in the printed parts, especially if they have thin walls. Binding the parts to a rigid base might reduce this curling effect, although it will require more post-printed processes to finish the part [18].

Finally, the most common method used to reduce the loss of material properties is the mixture of used powders with virgin ones. Normally, refresh rates of 50% are used in this technique, allowing the preservation of the powders properties. Studies differ in this method, where some authors defend that the partcake material should not be reused and others state that this material can indeed be reused but regular check-up tests must be done to assess its viability. A common test used to do a check-up is the Melt Flow Rate (MFR), which in the case of PA12 must be maintained above 18 g/10 min, otherwise, powder must be discarded [14], [18].

The degradation of polymers, or aging, is defined as any change in the molecular, supramolecular, or structure of the material that leads to an irreversible decrease of its properties and reduces its useful life service duration. This degradation phenomenon can occur in various ways, depending on one of two factors: internal or external [21], [22]. The external causes of degradation are considered to be physical and chemical interactions with the material and its surroundings, for example, weathering, UV radiation, humidity, and temperature, the latter being the most notable degrading agent in this technique. The internal causes are described to be thermodynamically unstable states present in the material, that if activated, usually by thermal stress, lead to a measurable change in properties. Examples can be unstable crystallization states, residual stresses, and incomplete polycondensation [21]–[23].

According to the literature, for polyamides, namely PA12 used in SLS, the main degradation phenomenon noticeable is the cross-linking of polymer chains caused by oxidation which is said to be dominant at the beginning of the degradation process, even when an oxygen-free environment is used. The main consequences of this problem are a decrease in flowability of the powder, due to an increase in molecular weight, and poor mechanical properties, especially strain at break and maximum stress [14], [24].

Chain scission also occurs in later stages of the SLS process, causing a decrease in molecular weight, that is counterbalanced with the increase of molecular weight cause by cross-linking. Studies also showed that this increase of molecular weight, and consequently decrease of flowability of the powder, affect the quality of manufactured parts, both in the correct development of the powder bed and the reproducibility of the manufactured component properties. Furthermore, the increase of molecular weight can be explained by linear growth or post condensation reactions. This increase can also lead to a shift of crystallization temperatures to lower values due to the lack of chain mobility. Although, this broadens the processing window, higher molecular weights mean higher viscosities, which prejudices the spreading of the powder and makes the SLS printing process harder [25].

Other factor that might influence the behaviour of the material, is the orientation in which parts are printed. Tomanik et al. [26], studied the differences in mechanical behaviour of PA12 printed samples with different building orientations to the building table, 0°, 30°, 45°, 60°, and 90° (0° being horizontally parallel to the building table and 90° being perpendicular from the building table). They discuss that the samples printed at 0° present the most ductile behavior and the 45°

the most brittle behaviour. The samples printed at 0° also showed tensile strength and elongation at break close to the parameters of the powder supplier while the other orientations did not. However, none of the orientations presents a Young Modulus close to the indicated by the supplier, being the 0° orientation the one closest to it, with a 15% lower value. This might suggest, that the most reliable way to print in SLS technology, is horizontally to the building table, and that this parameter is to be considered when printing.

2.5. Prediction of property loss method

In the literature, there is already a proposed methodology that aims to predict the property loss of polymers subject to reprocessing through primary recycling processes, such as injection molding, where the virgin polymer is processed, recycled (reground), mixed with virgin polymer, and reprocessed.

This methodology, developed by Bernardo et. al [27],for injection molding, where he reused the material injecting it through various cycles, granulating it after each ne and mixing it with virgin material, was able to predict the value of property decay for several properties, such as mechanical properties and melt flow index having only two simplifying considerations in mind: i) the regrind process does not affect the property of the polymer. ii) quantity of the virgin polymer added in each cycle is always the same.

The use of Bernardo´s methodology starts by obtaining the degradation curves, as can be seen in Figure 3, shows different degradation curves for different materials and properties, and illustrates the deterioration with the increase in the number of reprocessing cycles. This kind of curves are obtained when no virgin material is added to the reprocessing process. Applying a single-pass property value loss. Equation (1) for properties that follow a power-law, or equation (2) for properties that decay linearly. Each cycle until the nth cycle allows the construct of the type of degradation curve the property follows, that is later adjusted until an equation for P_n^* is reached. This information can later be used with a group of the equations called the law of mixtures, to predict the decay of properties when using blends of the used and virgin polymer [27], [28].

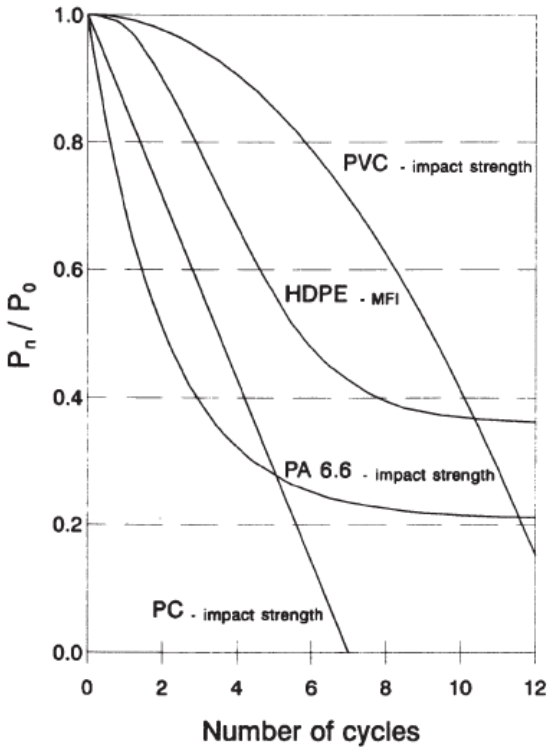

Figure 3 - Examples of degradation curves for various polymers and properties, from [27].

$$P_n^* = c\bar{P}_{n-1}^z \qquad equation\ (1)$$

$$P_n^* = c\bar{P}_{n-1} \qquad equation\ (2)$$

Although the differences between the SLS powders reprocessing and that corresponding to injection moulding, an attempt will be done to apply Bernardo´s methodology to SLS powders. Considering the regrind process (that takes place in injection moulding reprocessing) similar to the filtration process occurring in the powders reuse, this method might be considered for the prediction of properties of the reused powder. Figure 4 shows the reprocessing process of SLS

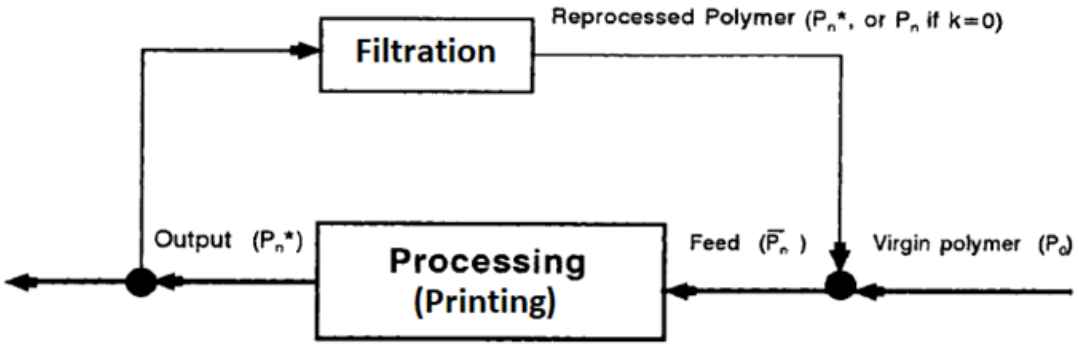

Figure 4 - SLS reprocessing cycle, adapted from [26].

where $P_0, \bar{P}_n$ or P_n^* are the properties of the virgin polymer, at the inlet of the reprocessing and at the outlet of processing respectively, and k is the fraction of virgin polymer added in each cycle, which in this case is zero and, as such, $P_n^* = \bar{P}_n$. In order to be able to apply this methodology, the decay of the properties characterized in this thesis have to follow one of the decay models considered by Bernardo [27].

Lopes et. al [29], succeeded in using Bernardo's methodology in predicting the decay of mechanical properties of PA12 powders used in SLS, such as the elastic modulus, tensile stress at yield, and tensile stress at break. Testing 5 cycles of reprocessing, only considered the fitting for the linear law of mixtures, through a custom-made software that, after 10 000 iterations, adjusted 3 different models and predicted the decay for the first 20 cycles of reprocessing. They reached the conclusion, that the mechanical properties and the mass of the material is compromised when only reprocessed material is used even at earlier stages of reprocessing. Another conclusion reached by then, is that this loss of properties can be minimized as the virgin powder incorporated in the mixture increases.

CHAPTER 3 – MATERIALS AND METHODS

3. Materials and methods

In this thesis, samples were produced through 3D printing of the PA12 powders through the SLS process with a successive increase in the number of cycles. Thereafter, samples were analyzed through different characterization methods. Lastly, the prediction method mentioned above was considered as a way for property prediction of the PA12 powder.

3.1. Materials and equipment

3.1.1. PA12

PA12-L 1600 powders, from *Prodways Technologies* were used to produce the different samples. Table 1 shows some of the properties of *PA12-L 1600*, and its datasheet can be seen in *Annex I.*

Table 1 - *PA12-L 1600* properties.

Property	Value	Unit
Bulk density	0.48	g/cm^3
Density of parts	0.95	g/cm^3
Melting Point	183	°C
Tensile strength	46	MPa
Tensile Modulus	1602	MPa
Elongation at break	36	%

3.1.2. ProMaker P1000

The equipment used for the samples production cycles was *Prodways technologies, ProMaker P1000* (Figure 5). The main equipment´s specifications are listed in Table 2 and the datasheet is included in *Annex II*.

Table 2 - General properties of the *Promaker P1000.*

Specification	Value	Unit
Max. build volume	300x300x300	mm
Laser power (CO_2)	30	W
Max. temperature	200	°C
Precision	0.02	mm

Figure 5 - *ProMaker P1000* : a) closed, and b) open.

The parameters used in all the printing runs were fixed and, were chosen based on *NM3D Ibérica* knowledge, being those used for their prints, as follows:

- The heating and cooling stages have a 90 min duration, while the printing takes 9 h* roughly (warm-up and cooling considered). The starting temperature was room temperature and the finish temperature for the cooling stage is 100 °C. The cooling stages were performed in the equipment, after the 100 °C value is reached the chamber can be opened (the equipment turned off) and the material can cool until room temperature in contact with the air without the risk of warping the printed parts.
- Both feeders (left and right) were set at 135 °C and will cool down until 100 °C at the end of the printing process. Pistons were set for 153°C.
- The building table printed at 180 °C and also cool until 100 °C.
- The purge gas (Nitrogen) was supplied at 120 °C.
- Layer thickness and recoater speed were 0.1 mm and 140 mm/s, respectively.
- Relaxation delays** were set for 3s for the recoating delay and 2s for the sintering delay.
- The laser parameters were divided into two sections, namely the parameters for the infill of the parts and the parameters for the outline of the parts. On the infill, laser power was set for 14 W and the laser beam offset for 0.75 mm, the hatching distance is 0.2 mm for both X and Y directions. The outline laser power was 10 W, and the laser offset is 0.54 mm. The overall laser speed was 3.5 mm/s.

* The printing time was obtained by the addition of parts to the building space, until the 9 h value was reached. These parts had commercial and practical use for the company. Although different

parts were added each print, the samples were always printed in the same coordinates of the building table.

** Relaxation delay is the time in which the equipment does nothing to ensure the powder is in equilibrium (having relaxed process induced stress) before any action takes place. In the case of recoating delay, it is the time between the recoater making the powder bed and the laser starting sintering. The sintering delay is the time between the laser finishing the sintering and the recoater making the next layer of the powder bed.

3.1.3. Additional processing equipment

The powders filtering was performed in the *ProTool BS01* equipment (Figure 6), from *Prodways Technology*, and the "powders mixing" promoted to enhance the powders homogeneity was done in a simple mixer with 3 rotational blades (Figure 8). Lastly, for sample part cleaning, sand jet equipment, the *Guyson Formula 1400* (Figure 7), from *Prodways Technologies*, was used.

Figure 6 – Filtering machine used, *ProTool BS01*.

Figure 8 - Rotational mixer used for powder "mixture".

Figure 7 - Sample cleaning equipment, *Guyson Formula 1400.*

3.2. Methods

To be able to study the effects of degradation in the material, the first cycle of processing was printed with 100% of virgin material, then every cycle was performed with 100% of recycled powders from the previous one (to ensure there was enough powder for all the cycles processed, the equipment was loaded to the maximum capacity on the first processing, even though there was only a portion of that powder used). The original plan was to reprocess and characterize the powder in 12 cycles (the recommended by suppliers) and that was the case for most of the characterizations made. However, the mechanical tests made in the first attempt were unsuccessful and the samples were lost. To still study this part of the characterization, a new batch

of samples were printed but only until reprocessing cycle number 6, with material given by the collaborating company.

The process, consisted in the printing of the samples (and parts already explained), then cleaning of those, then filtering of the remaining unsintered powder which consists in making the powder pass through different sieves with ceramic balls and a filter were some of the powder remains trapped and it is discarded, followed by 2 minutes in the rotational mixer to promote homogeneity, collecting of powder samples and the repetition of the whole process. For the first cycle, the virgin powder must also be filtered to guarantee its particles are completely lose and there are no agglomerations that might be formed during transportation and storage.

3.2.1. Powders

After each printing, the powders were filtered, followed by 2 minutes in the rotational mixer to promote homogeneity just like the virgin powder. After this pre-printing process was concluded, around 250 g of the partcake powders were collected and stored in a tight bag to avoid moisture contamination.

3.2.1.1. Powders characterization

Differential Scanning Calorimetry (DSC)

DSC is a technique for the thermal analysis of polymeric materials. It is based on the measurement of the difference in heat flow between a sample and a reference as a function of temperature. This technique is able to accurately determine any characteristic in the material that causes a variation on this heat flux rate, such as, melting and crystallization temperatures, thermal parameters of chemical reactions, heat capacity, and others [30].

This test was made to determine the value of the melting peak, which provides information about the melting point and the area underneath that peak, which provides information about the melting enthalpy. With the melting enthalpy value, conclusions about the degree of crystallization of the powders will be clear, and the influence of said degree in the melting point will be clear.

The energy changes measured by the DCS equipment can be obtained during heating or cooling of the sample, or even by holding it isothermally. A big advantage of this technique is the fact that the samples need little to no preparation for measurements and also the quantity of material used for each sample is in the few milligrams [31].

DSC analysis were performed in NETZSCH *DSC 200 F3* (Figure 9). Two heatings were programmed. The first heating was performed to eliminate the thermal history of the samples and to ensure that, for example, humidity did not affect the measurements. The second heating was conducted to obtain the required results. The purge gas was nitrogen, purged at 50 ml/min, ensuring an inert environment for testing.

The samples were weighed on a scale with ± 0.001 mg precision, and placed in an aluminium crucible, also from *NETZSCH*. The lid of the crucible was punctured to ensure the gases released during the material melting could escape without disturbing the test. Figure 10 shows the sample crucible and also the disposition of this crucible and that of the reference one in the equipment.

Due to the availability of the DSC equipment, it was not possible to analyse all 12 cycles printed. As such, it was analysed a sample of virgin powders, and samples from 8 different prints, those being prints 1, 2, 3, 6, 9, 10, 11, 12.

The thermal cycle used for testing is as seen in Figure 11.

Figure 9 - DSC equipment used, *NETZSCH DSC 200 F3.*

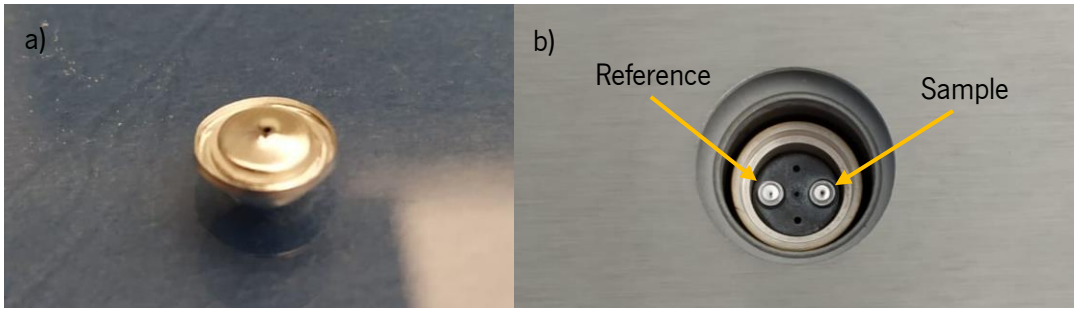

Figure 10 - a) Crucible with sample ready to be tested b) disposition of the crucibles in the equipment oven.

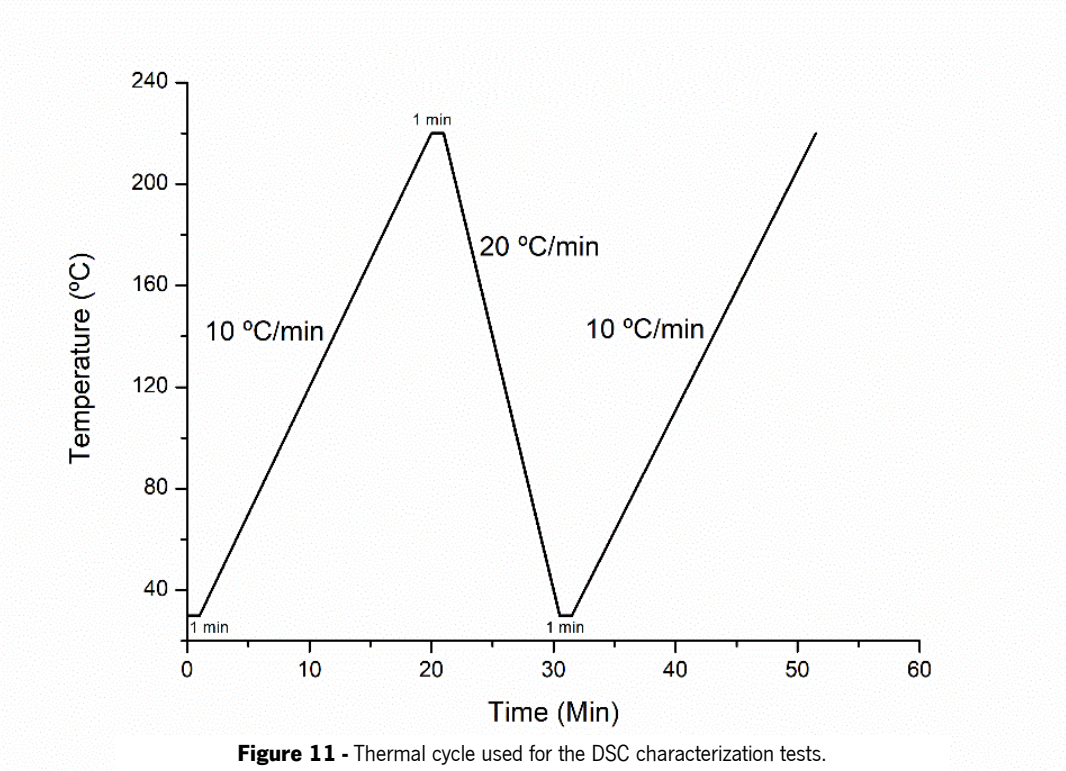

Figure 11 - Thermal cycle used for the DSC characterization tests.

Scanning Electron Microscopy (SEM)

SEM is a characterization instrument widely used in various research fields. Through an electron gun, a high-energy laser beam is generated, in a vacuum environment, and electrons are accelerated and collide with the surface of the sample. This collision emits various types of radiation that can provide different information, the most common types being the information obtained from secondary electrons (SE) and backscattered electron (BSE). These vary with any alteration of surface topography, being able to depict a high-resolution image of the surface of the sample. Besides these types of electrons, SEM can also provide information through characteristic X-Rays and photons of various energies, which provide crystallography and chemical composition information [32]–[34].

Usually, SEM instruments have an energy dispersive X-ray system (EDS) embedded in them. This system, simultaneous with the SEM, can produce a chemical analysis of the sample region observed in the SEM monitor. As the name suggests, this technology uses X-rays to identify and quantify the elements presented in the sample, giving valuable information about what reactions might have happened in it, for example in degradation or failure analysis [35].

The powders morphology was accessed by *NanoSEM – FEI Nova 200* with an integrated EDS system *EDAX – Pegasus X4M.*

3.2.2. Printed samples

Each printing cycle produces samples for additional characterization, which were be divided into two types. i) The samples for mechanical characterization (tensile tests), following the geometry of the standard *DIN 53504-S3a* (Figure 12-a)), that were printed in two different orientations, vertical and horizontal to the building table for prints 1 to 6; ii)the samples for the porosity analysis, a small cuboid-like shapes ((5x5x20) mm^3), always printed vertically (Figure 12-b)) were analysed for printing cycles number 1, 4, 8, and 12. The tensile test samples, were printed inside 2 cages,

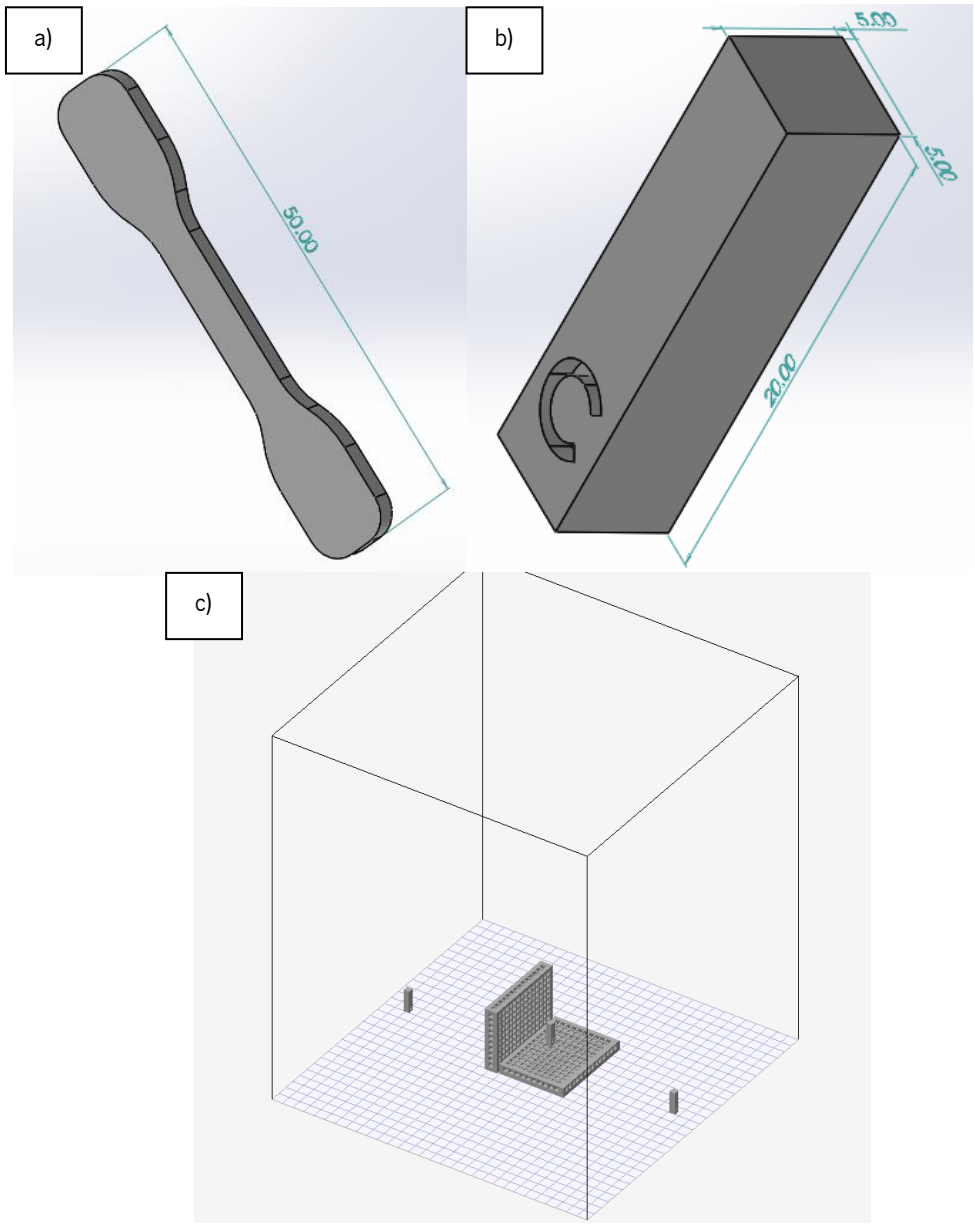

Figure 12 - a) Tensile sample *DIN 53504-S3a.* b) CT sample. c) Disposition of the samples in the SLS equipment for all cycles.

marked to distinguish the vertical and horizontal ones. The disposition of the samples in the printing equipment is presented in Figure 12-c).

3.2.2.1. Samples characterization

The characterization of different printed samples and the equipment used in such characterization are as follows.

Tensile tests

Tensile tests are widely used both in investigation and in industrial applications to obtain essential information about the mechanical properties of materials.

Shimadzu AG-X tester was used for tensile tests (Figure 13). The tests were performed until break of the samples. Tensile samples from prints 1 to 6 were analysed, for the horizontal orientation of printing, 7 samples per print were considered, and for the vertical orientation only prints 1, 3 and 6 were considered and 7 samples per print were also used, for a total of 63 samples. The

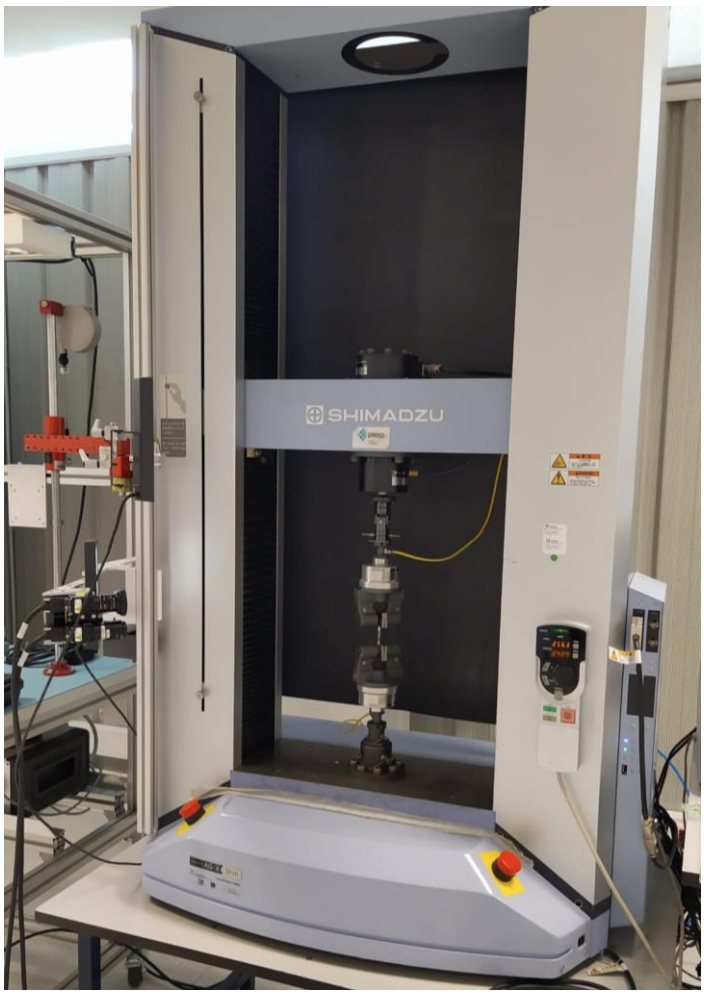

Figure 13 - Equipment used for tensile testing, *Shimadzu AG-X* with video extensometer.

deformation and elastic modulus were obtained through a video extensometer. The parameters used are described in Table 3.

Table 3 - Parameters used in the tensile tests.

Parameter	Value	Unit
Load cell	1	KN
Test speed	5	mm/min
Gauge length (jaws)	20	mm
Gauge length (extensometer)	Variable	—

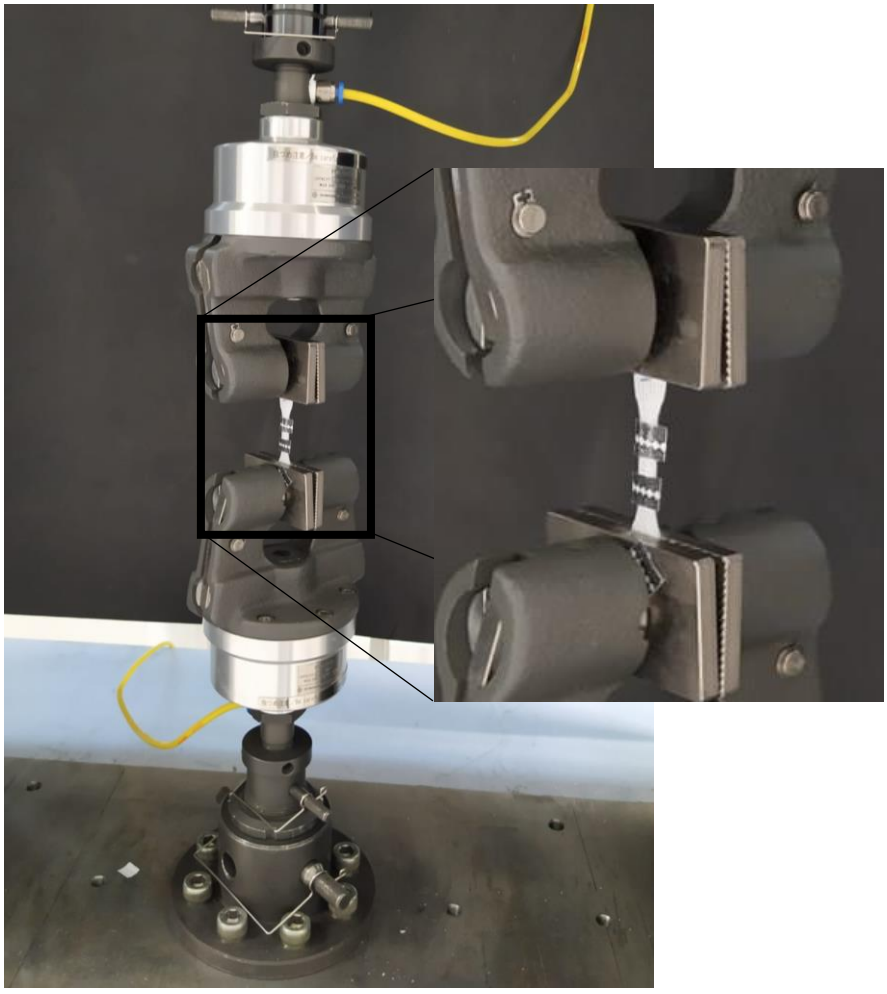

Figure 14 - Preparation of the test piece for tensile testing.

Computed tomography (CT)

CT uses X-rays to analyze the samples, these are generated in a vacuum tube where electrons are freed from a cathode, usually in the form of a filament, through heating this material utilizing an electrical current. Then by applying a high voltage, these electrons are accelerated towards an anode target. Most of the kinetic energy in this process is transformed into heat, although some of it is converted into X-rays (about 1%). Therefore, the anode presents high temperatures, and some

sort of cooling system has to exist to prevent it to overheat and melt. When the electron strikes the target, X-ray photons are produced and aimed at the sample [36].

Once the photons reach the sample, different kinds of interaction may occur (Figure 15), and with these interactions, namely the absorption and scattering, their energy will emerge from the sample with different attenuation intensities and be measured by a detector. These measurements will allow the equipment to create images (radiographic images) proportional to the X-ray photons detected, and through the combination of these images taken in a 360° rotation of the sample, a 3D image of the internal and external features is constructed allowing for characterizations such as detailed measurements and porosity calculation [36].

Samples (Figure 12-b) were analysed in the equipment *XT H 225 ST* (see Figure 16), from *Nikon Metrology,* using a tungsten filament, for prints number 1, 4, 8, and 12*.* The scans were performed all around the sample, rotating it 360°, with beam energy of 180 kV, beam current of 11 μA, 20 W of power, and exposure of 4 fps. Two frames were taken for each thesision. All data was analysed in the software *Visual Graphics Studio.*

Reprocessing cycles were evaluated with 3 test pieces (TP) printed vertically in each cycle (one on each side of the printing table, left and right, and one on the center). For availability reasons of the equipment, only prints 1, 4, 8 and 12 were analysed for a total of 11* samples. For each TP, 3 longitudinal cuts (see Figure 17) were made (at 1 mm, 2.5 mm, and 4 mm from the sample reference wall**), and 4 values of porosity were obtained in each section (a total of 12 values per piece) in order to obtain a representative porosity value for each printed part. Also, 3 transversal cuts (see Figure 18) were made to confirm the shape of the samples.

*See note in page 43.

**Sample reference wall is the wall with the letter that indicates the zone were it was printed, center, right or left side of the building table.

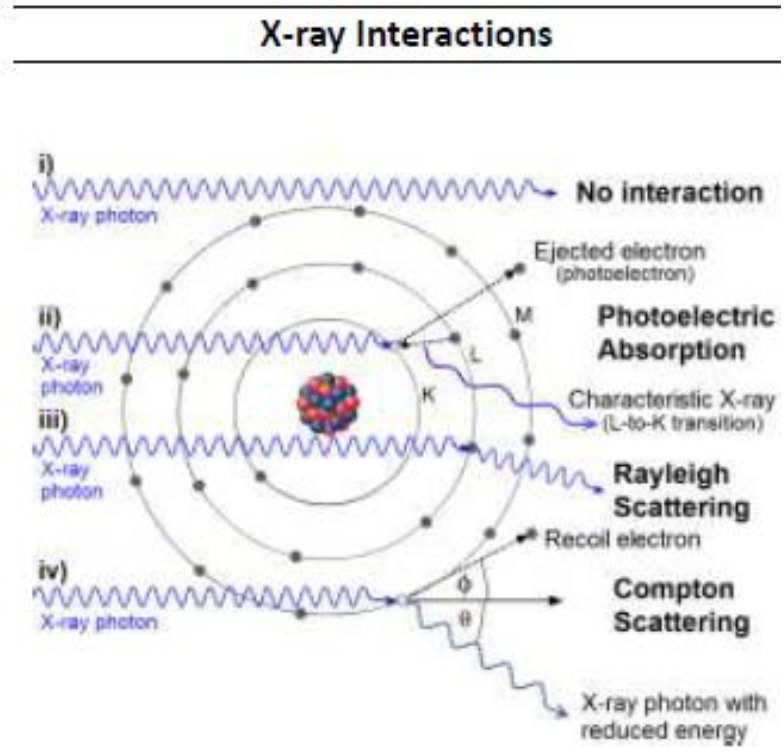

Figure 15 - Different types of interactions between the X-ray photons and atoms of a sample from [35].

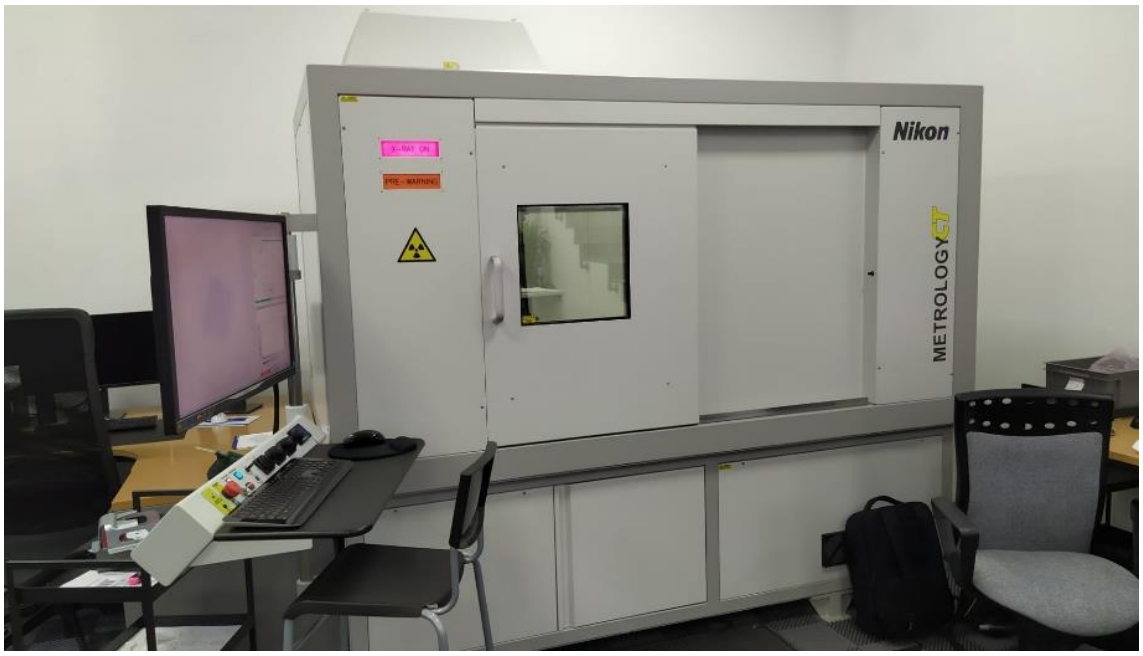

Figure 16 - CT equipment used, *XT H 225 ST.*

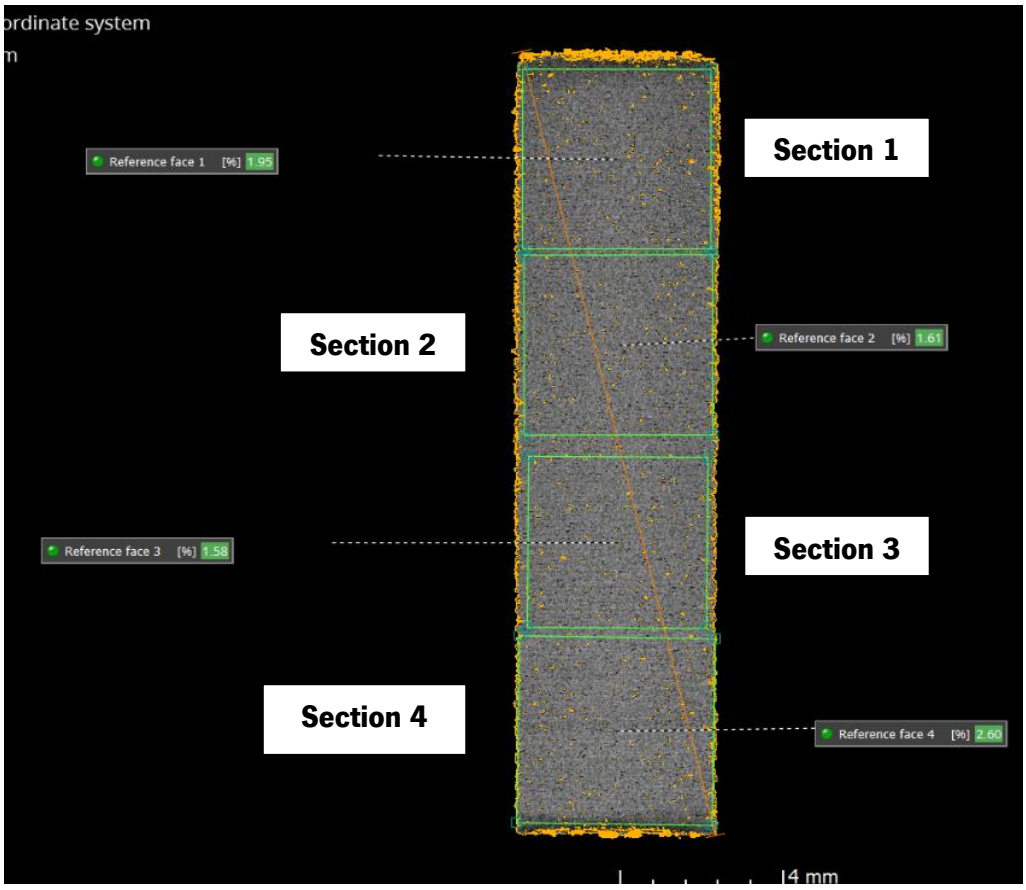

Figure 17 - Example of the longitudinal cuts made and the 4 sections where porosity values were taken.

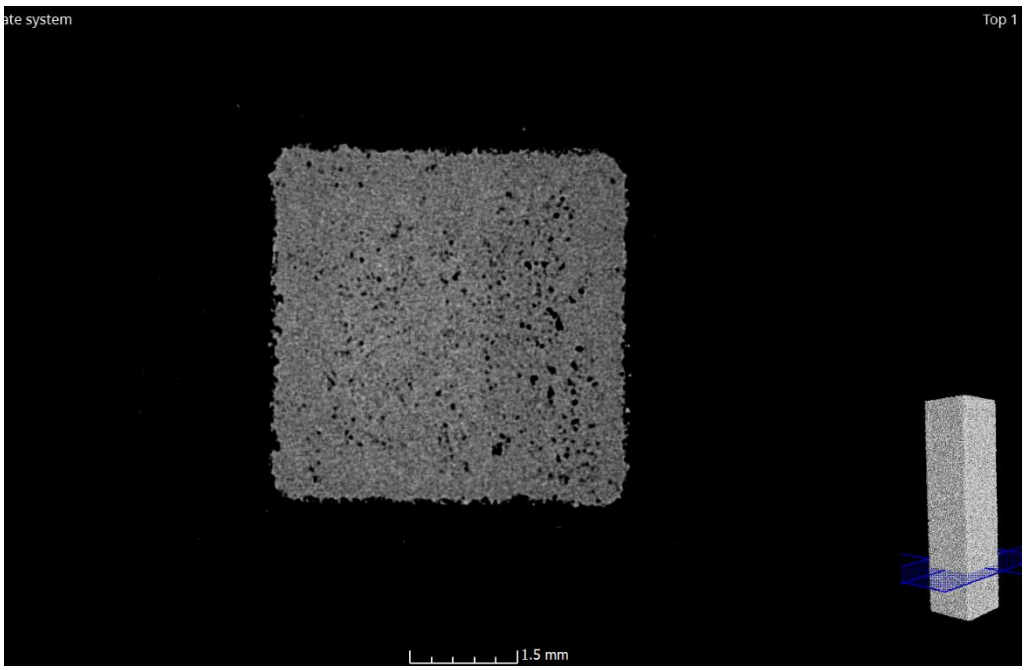

Figure 18 - Example of the transversal cuts made for shape verification.

3.2.2.2. Statistical analysis

The results are presented as the average ± standard deviation values from seven independent samples. Statistical analysis was evaluated by one-way ANOVA followed by Tukey's test for multiple comparisons, considering $p < 0.05$ as significant.

3.2.3. Visual analysis

During the successive printing runs, a visual evaluation is made to access the visual quality of the parts throughout the reprocessing cycles. This visual interpretation is important due to the fact that this technology is widely used in RP where, good surface finishing is required.

Chapter 4 – Results and discussion

4. Results and discussion

4.1. Powder characterization

4.1.1. Differential Scanning Calorimetry

The DSC curves maintain, for all printing cycles evaluated, the same trend, which means there are no new transformations occurring in the material as the cycles progress. Figure 19 and Figure 20 show a representative example of the overall curves obtained in each testing and a close-up of the second heating curve. Also, it is worth mentioning that during heating, more specifically during the second heating, the material presents a slight exothermic peak that indicates a crystallization right before melting begins, at temperatures between 160 °C and 165 °C. This crystallization occurs basically at the same level throughout the different printing cycles as can be observed in Figure 22 and Figure 21. This transformation might be explained due to the fact that during the cooling the material could not crystalize in all its totality and, as above the glass transition temperature the molecular chains have high mobility, they tend to form ordered arrangements, creating crystals, originating this phenomenon [37].

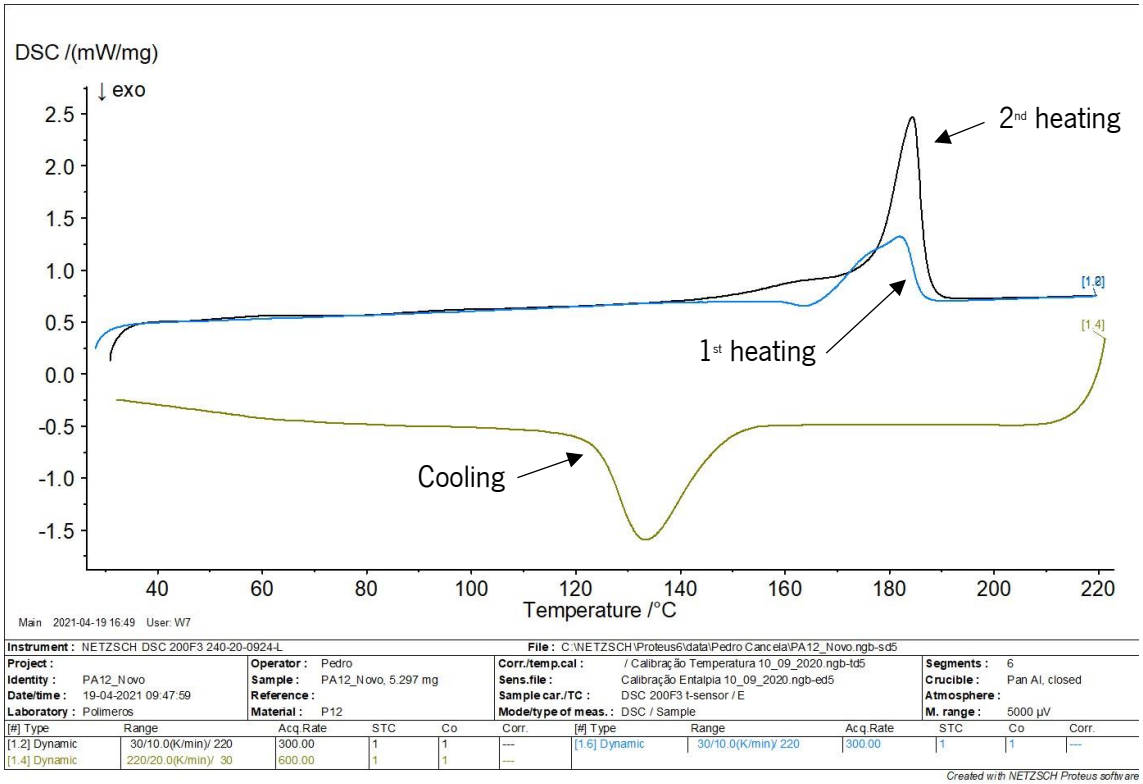

Figure 19 - Example of the overall results obtained in DSC testing (virgin powder).

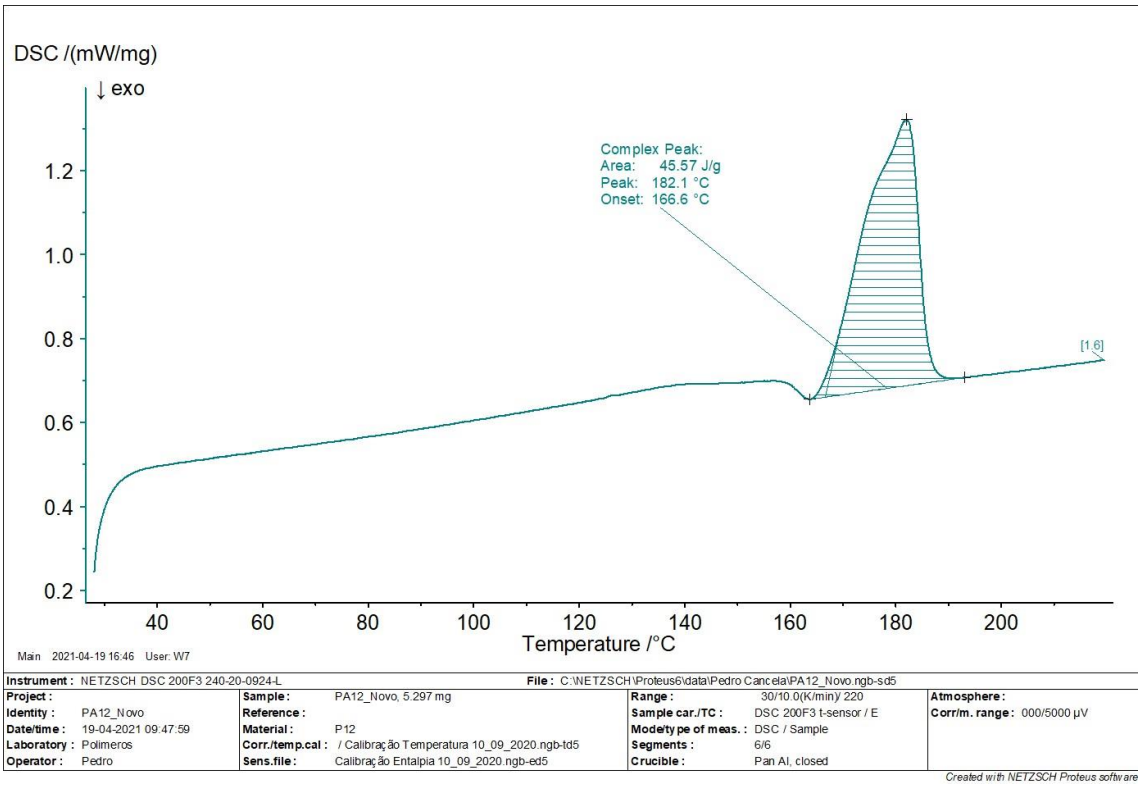

Figure 20 – Close up of the curve obtained in the 2nd heating of DSC testing cycle (virgin powder).

These results are presented in Figure 23 to Figure 26 for both the first and second heating of the samples. The most accurate way to understand and compare these results is to analyse the second heating, as the samples are all in the same stable state with all the thermal history erased. It is evident that the material suffers degradation through its reprocessing cycles because its melting enthalpy decreases at a constant rate from values of 45 J/g to values close to 41 J/g (a drop of about 9% of the original melting enthalpy), suggesting that there is a lower degree of crystallinity in successive cycles, resulting also in a decrease of approximately 5 °C in the melting temperature. This suggests that chain-scission might be happening due to the thermal conditions imposed by the SLS process. Thermal degradation usually affects the polymers by activating depolymerization reactions, meaning that breaking of the main chain might occur. This happens due to the stress intra-chain bonds are subjected to, because the heat amplified intramolecular vibrations, which causes them to break (chain-scission) originating fragments and radical end-groups [38], [39].

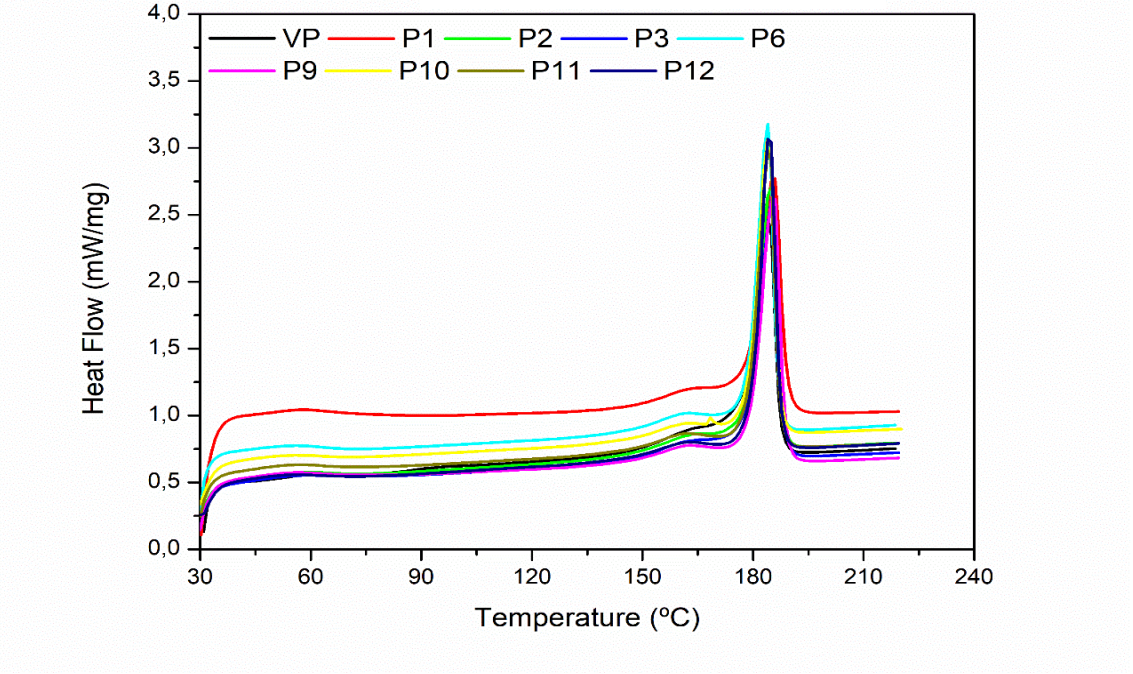

Figure 22 - Overlapping of the DSC curves obtained for the first heating for all tested samples.

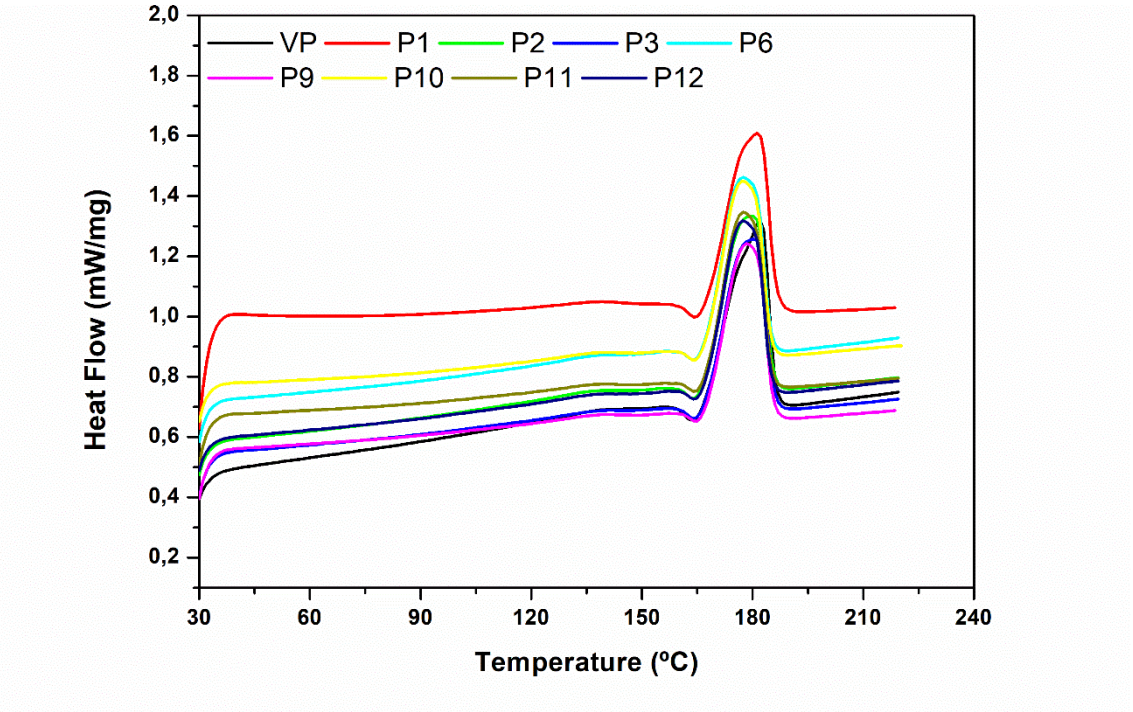

Figure 21 - Overlapping of DSC curves obtained for the second heating for all tested samples.

Although the second heating is the most used and accurate way to compare sample results, the first heating cannot be ignored as it is worth noting that even though the melting enthalpy decreases in both the first and second heating cycles, this fall is more severe in the first heating, dropping from values of 105 J/g to 90 J/g (more than a 14% drop), again suggesting a lower degree of crystallinity. However, the melting point remains constant for the most part, having just a 1.4 °C difference between the highest and lowest value registered (showing only a slight decrease) throughout all the reprocessing cycles. This might indicate that in the first heating, there might be some phenomenon that maintains the melting point of the material constant. And as in this heating, the thermal history of the samples is not erased, this heating can help to understand what actually happens in terms of degradation in this technology. As already mentioned in chapter 2, one reason for this might be the occurrence of cross-linking of the polymer chains in a greater way than the chain-scission leading to the maintenance of the melting point. As the SLS process does not possess second heating when printing, it might be necessary to maintain or even increase (as the highest value registered does not correspond to the virgin powder) the temperature of the SLS process to guarantee the correct printing of parts, a recommendation made by most suppliers. Both degradation mechanics describe might competitively occur in the powder, being cross-linking more dominant in the early stages of degradation and chain scission in the latter.

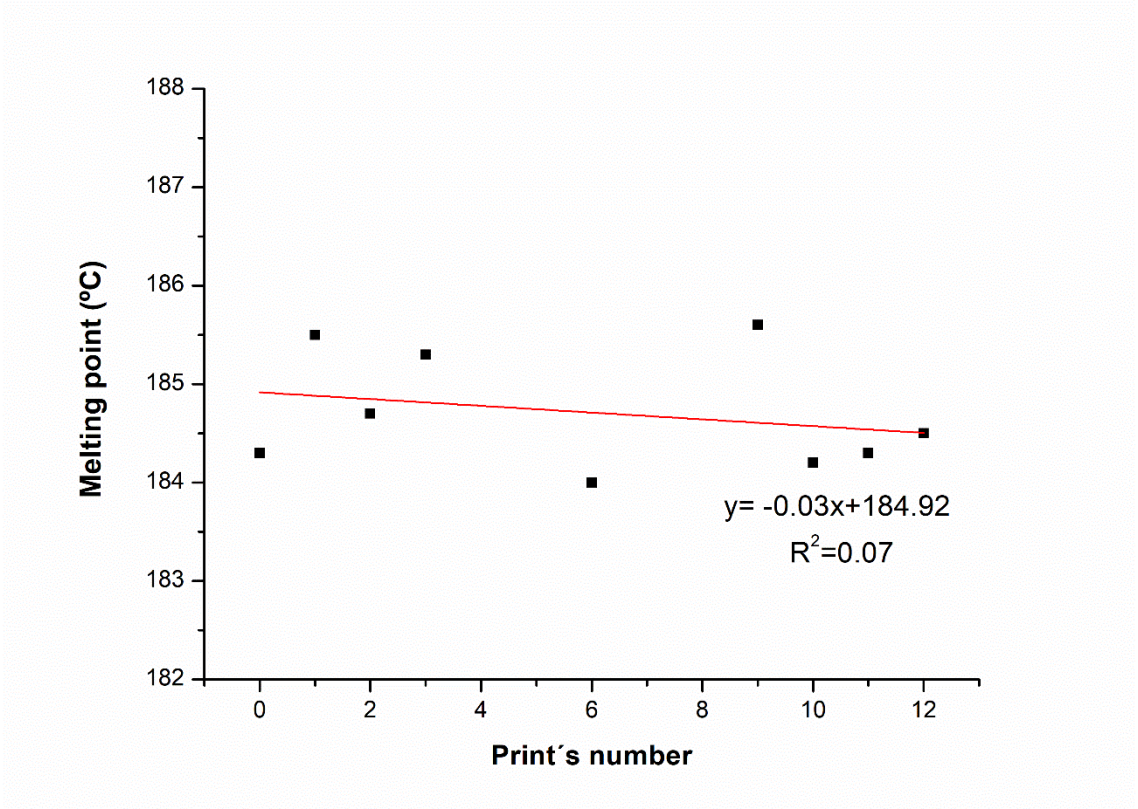

Figure 23 - Variation of the melting point in the first heating of the samples.

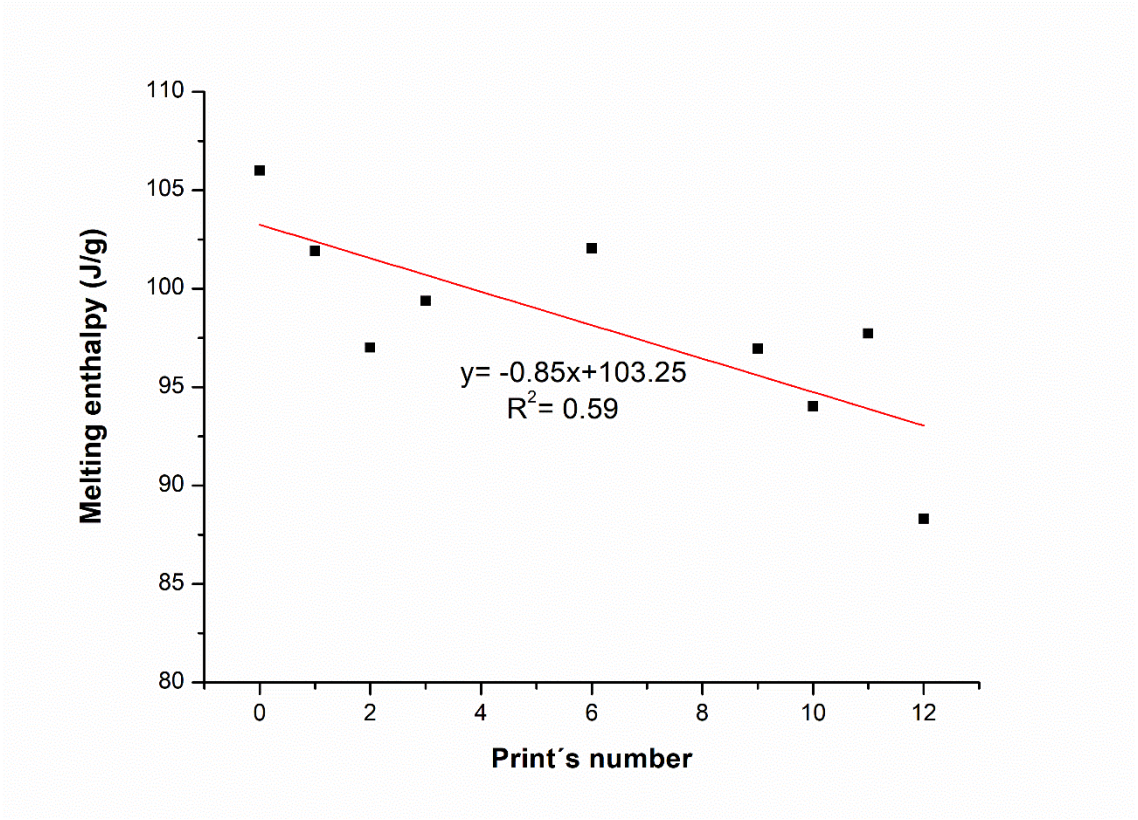

Figure 25 - Variation of melting enthalpy obtained in the first heating of the samples.

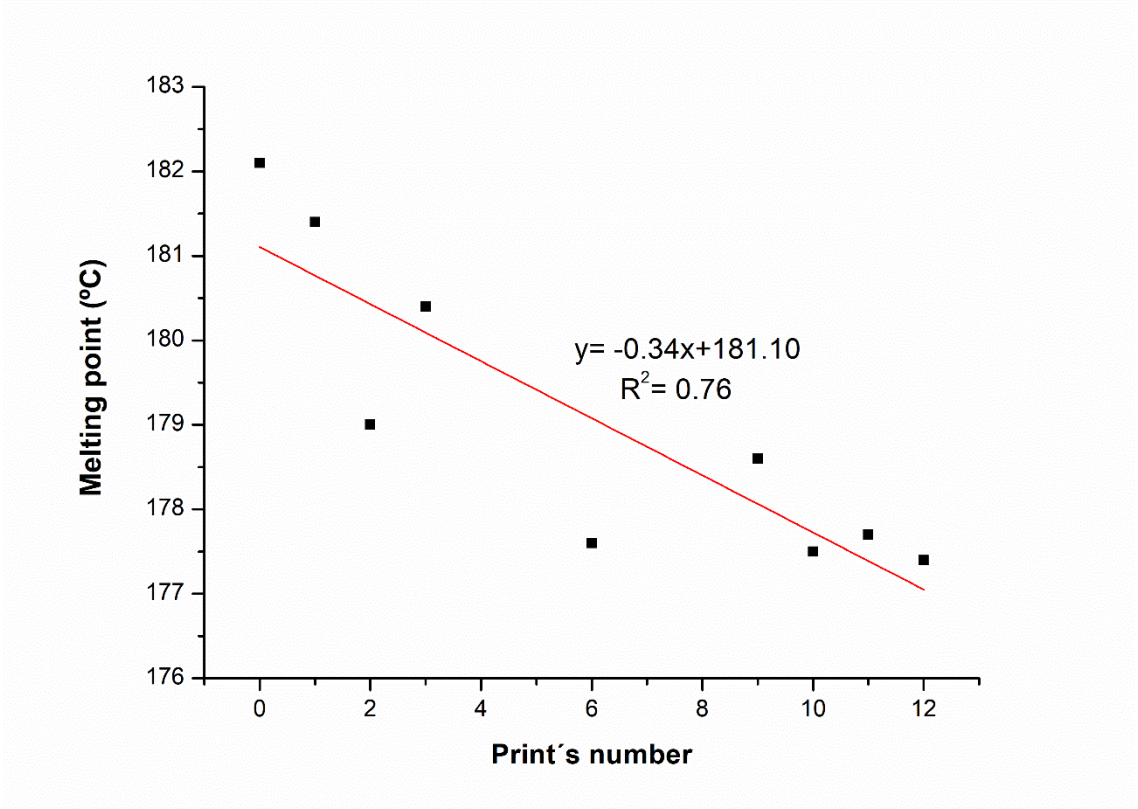

Figure 24 - Variation of the melting point in the second heating of the samples.

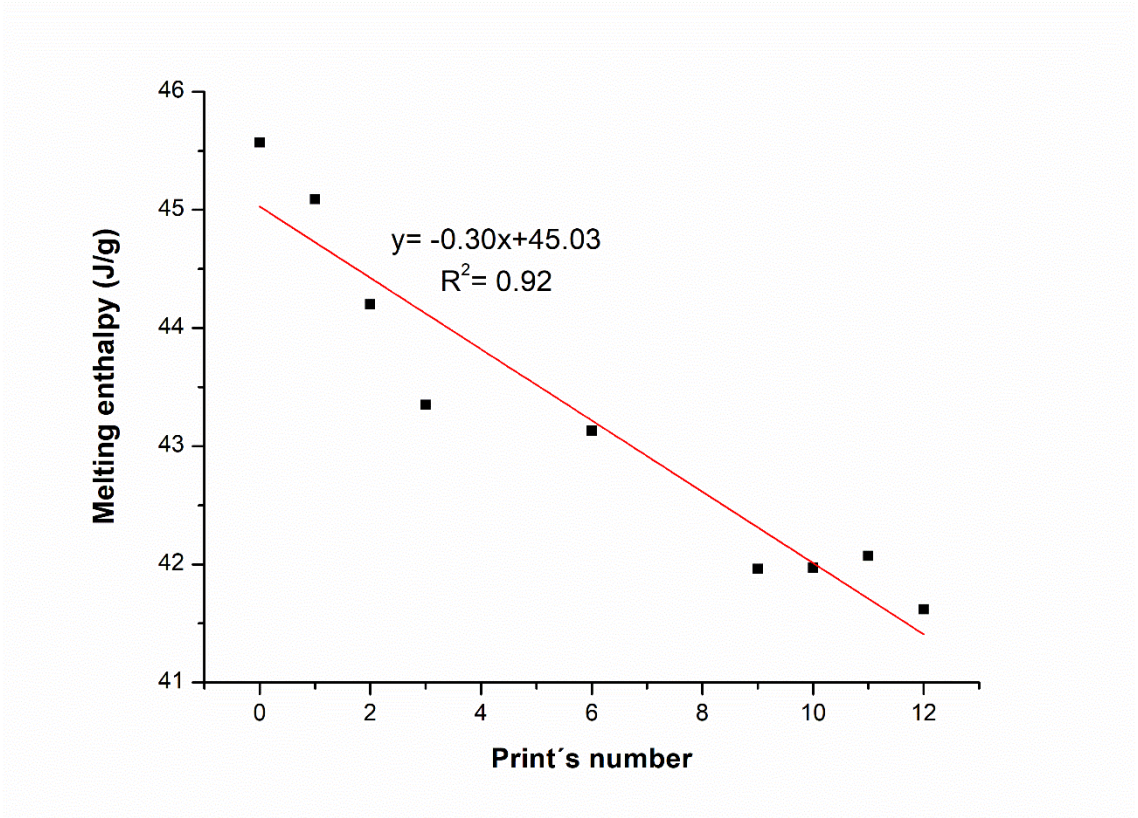

Figure 26 - Variation of the melting enthalpy obtained in the second heating of the samples.

Table 4 - Summary of the results obtained for the first heating in the DSC characterization.

Reprocessing cycle	Melting enthalpy (J/g)	Melting point (°C)
Virgin powder	106.00	184.3
Print 1	101.90	185.5
Print 2	97.01	184.7
Print 3	99.37	185.3
Print 6	102.04	184
Print 9	96.94	185.6
Print 10	94.03	184.2
Print 11	97.72	184.3
Print 12	88.32	184.5

Table 5 - Summary of the results obtained for the second heating in the DSC characterization.

Reprocessing cycle	Melting enthalpy (J/g)	Melting point (°C)
Virgin powder	45.57	182.1
Print 1	45.09	181.4
Print 2	44.20	179
Print 3	43.35	180.4
Print 6	43.13	177.6
Print 9	41.96	178.6
Print 10	41.97	177.5
Print 11	42.07	177.7
Print 12	41.62	177.4

4.1.2. Scanning Electron Microscopy

For the SEM analysis both virgin powders and powders from reprocessing cycle number 12 were chosen. Figure 27 shows the morphology of these powders.

From SE/SEM images it is possible to observe that the reused powder has a very different topography when compared to the virgin ones. The reused powders have not only a much rougher surface but also seem to present higher porosity. This is probably due to the successive heating cycles the powder was subjected to, and due to the filtration operation, the powder needs to go through after each print. This porosity in the powders might induce porosity in the produced parts. Which will be evaluated in greater detail in section 4.2.2. of this thesis.

The SEM equipment used had the capability of EDS analysis, as such, both samples were analyzed with this technique, being the corresponding results presented in Table 6. It can be seen that the only significant difference between both samples, is that the reused powder appears to contain a bigger percentage of nitrogen (even though the machine internal error fluctuates the values, and they might intercept). This means the powders might incorporate the nitrogen used as purge gas in its composition, and as the reused powder analyzed has gone through 12 printings, it built up the nitrogen incorporation quite significantly.

Table 6 - Weight percentages detected by EDS in both samples.

Sample	Element	Weight %	Int. Error
Virgin powder	C	75.19	0.65
	N	14.51	5.84
	O	10.30	3.66
Reused Powder (12 prints)	C	65.84	0.40
	N	22.68	2.44
	O	11.53	2.00

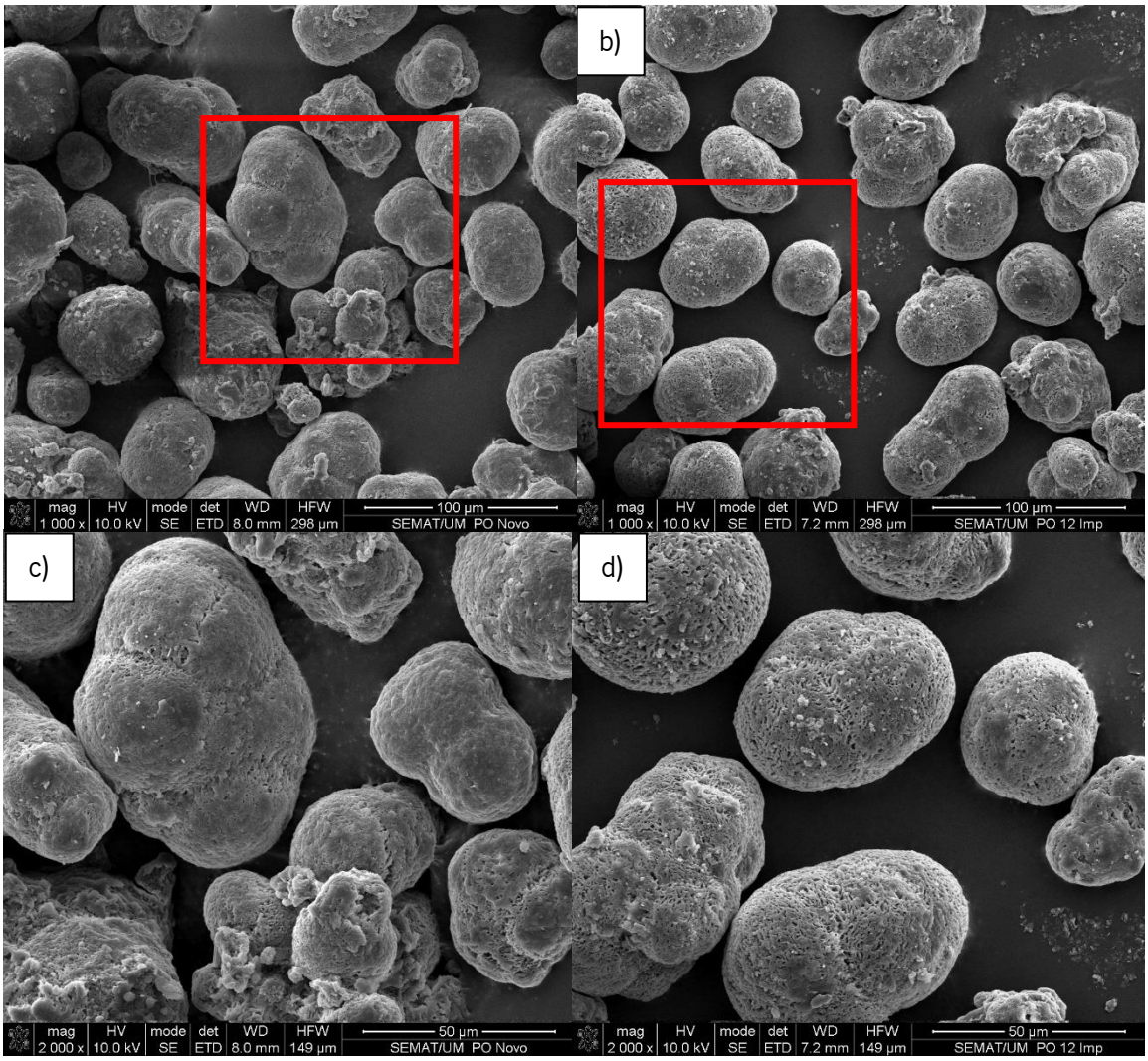

Figure 27 – SE/SEM images of a) and c) virgin powder and b) and d) reprocessing cycle 12.

4.2. Characterization of the printed samples

4.2.1. Tensile Tests

The tensile tests for each printing cycle may give information through the stress vs strain graphs of the prints, about the characteristics of the powder and properties of the printed parts throughout the recycling process. This characterization was carried out in samples corresponding to 6 consecutive cycles, printed with 2 printing orientations, horizontal and vertical. In the horizontal orientation, 7 test pieces (TP) were printed and analyzed for the 6 referred cycles. In the vertical orientation, also 7 TP were printed but only for the first, third, and sixth cycles, once prints produced in this orientation tend to fail at lower stress and strain values (when compared to those produced in the horizontal one). As a consequence, differences are less noticeable in successive cycles.

Figure 28 to Figure 34, show the mean results obtained in this characterization, where statistically homogenous groups are indicated by the same letters. As it can be observed in the comparison of the curves (Figure 28), the different orientations affect the behavior of the printed parts when subjected to the uniaxial force (as expected). The parts printed vertically present a much more brittle behavior, barely reaching the plastic domain of the stress vs strain curve before the break, while the parts printed horizontally present a ductile behavior. This is due to the adhesion between layers not being strong enough to sustain the high forces applied during the test, and in the case of vertical printed samples, these interlayer bonds are perpendicular to this force, breaking relatively early and causing the failure of the parts. The horizontal printed samples have these interlayer bonds parallel to the applied force, not affecting significantly the failure of the material.

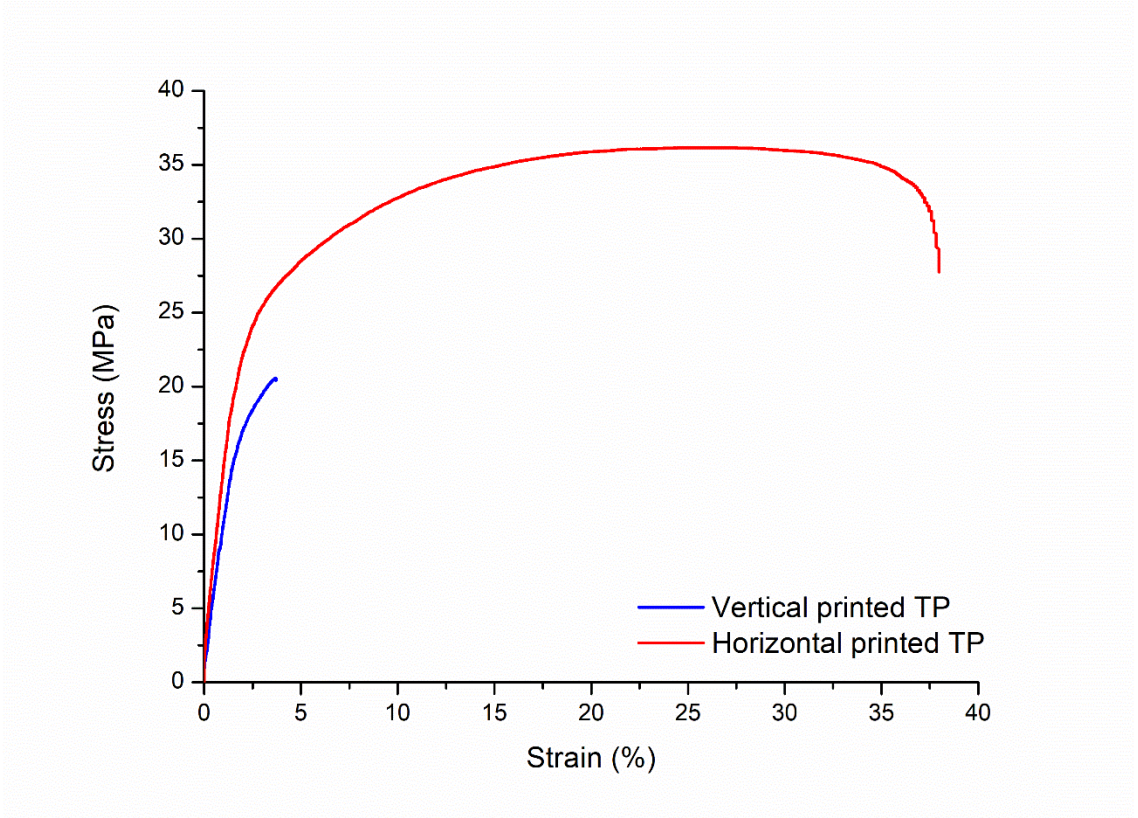

Figure 28 - Stress vs Strain curves of the TP printed horizontally and vertically.

Regarding the Young´s modulus, both printing directions have similar mean values, as seen in

Cycle and orientation	Young Modulus (MPa)	Strai at break (%)	Máx stress (MPa)
1H	1178.14±138.31	30.63±7.30	35.95±0.43
2H	994.98±128.51	31.20±9.76	35.42±0.60
3H	1306.87±205.39	32.82±8.56	34.23±1.95

4H	1131.78±287.59	29.76±6.30	36.48±0.22
5H	1021.98±312.92	19.33±4.87	29.35±0.40
6H	1156.76±318.55	36.26±9.28	35.28±1.39
1V	894.22±108.84	5.78±1.73	21.86±1.24
3V	1101.00±270.6	4.01±1.52	24.45±0.81
6V	1175.97±683.09	2.83±0.90	17.90±0.74

Table 7, (slightly different from the datasheet values, see ANNEX II) and through the one-way ANOVA and Tukey analysis, represented by the letters in Figure 29 to Figure 34, no statistically significant difference was observed for the mean values of this property. Thus, no significant dependence on printing cycle for the Young´s modulus was observed. The standard deviation is high for this property, especially for 6th cycle test pieces printed vertically, this reinforces what was already mentioned concerning the lower performance resulting from the vertical direction of printing, and evidence that this technology appears to have difficulties in reproducibility and repetitiveness.

Note: ANOVA and Tukey analysis, is represented by the letters and the asterisks in the graphics shown. When asterisk is shown, the groups have statistically significant differences between then. Also, when the letter differs between the groups, statistically significant differences are also apparent.

On the other hand, differences in the maximum stress measured are noticeable. Firstly, the horizontal TP reached higher values of maximum stress, as expected due to the already mentioned problems related with the vertical printing. Then, while in the horizontal orientated TP no statistically significant differences were obtained, in the vertical TP all the 3 cycles tested present a significant difference in mean values, with a slightly decreasing tendency for the last cycle. This means that throughout the printing cycles this property tends to be affected in a negative way.

Lastly, and in line with previous observations, the strain at break is much lower in the vertically printed TP, reaching a deformation of less than 8 %, whereas the horizontal TP, reach deformations of 40 %. The vertical printed parts follow the same trend as they did in relation to the maximum stress, with a slight decrease through the cycles, but only having statistically significant differences between printing cycles number 1 and 6. Horizontal test pieces showed that the strain is less

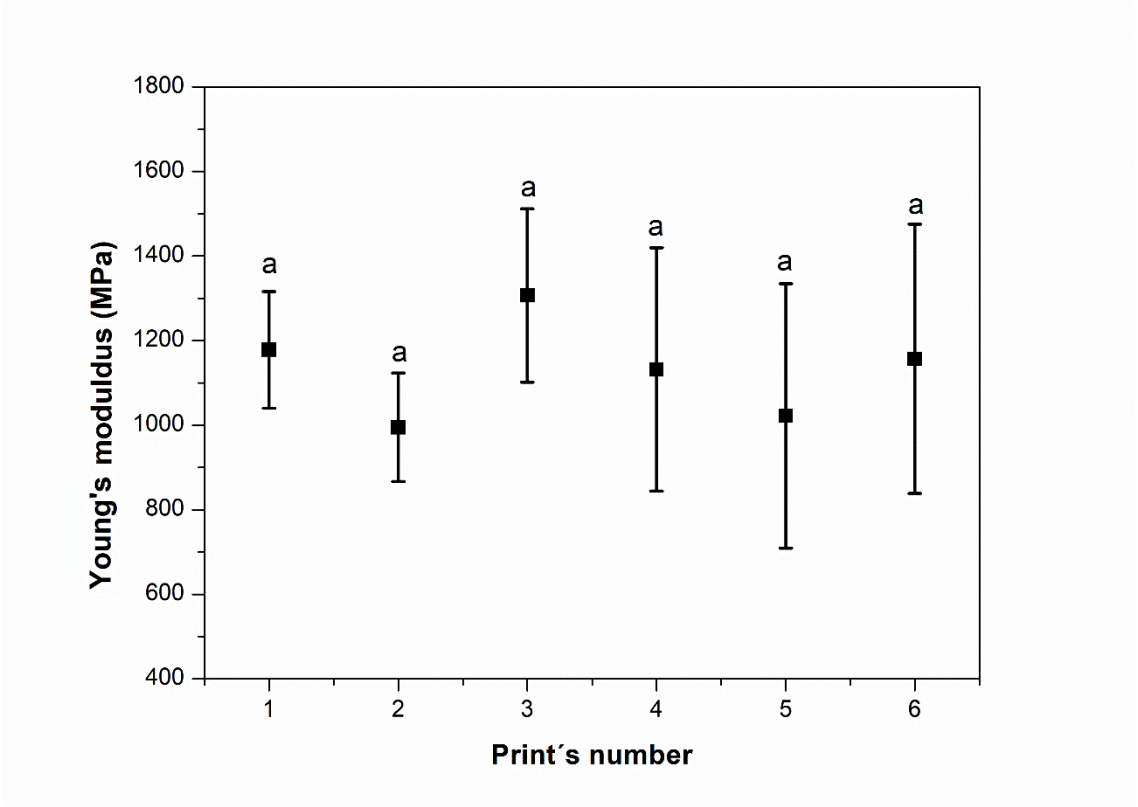

Figure 29 - Young´s Modulus through the reprocessing cycles for the Horizontally printed TP.

affected, presenting similar mean values, for the first 4 cycles. However, there are some statistically significant differences in mean values, namely between printing cycles 3 and 5 and between printing cycles 5 and 6.

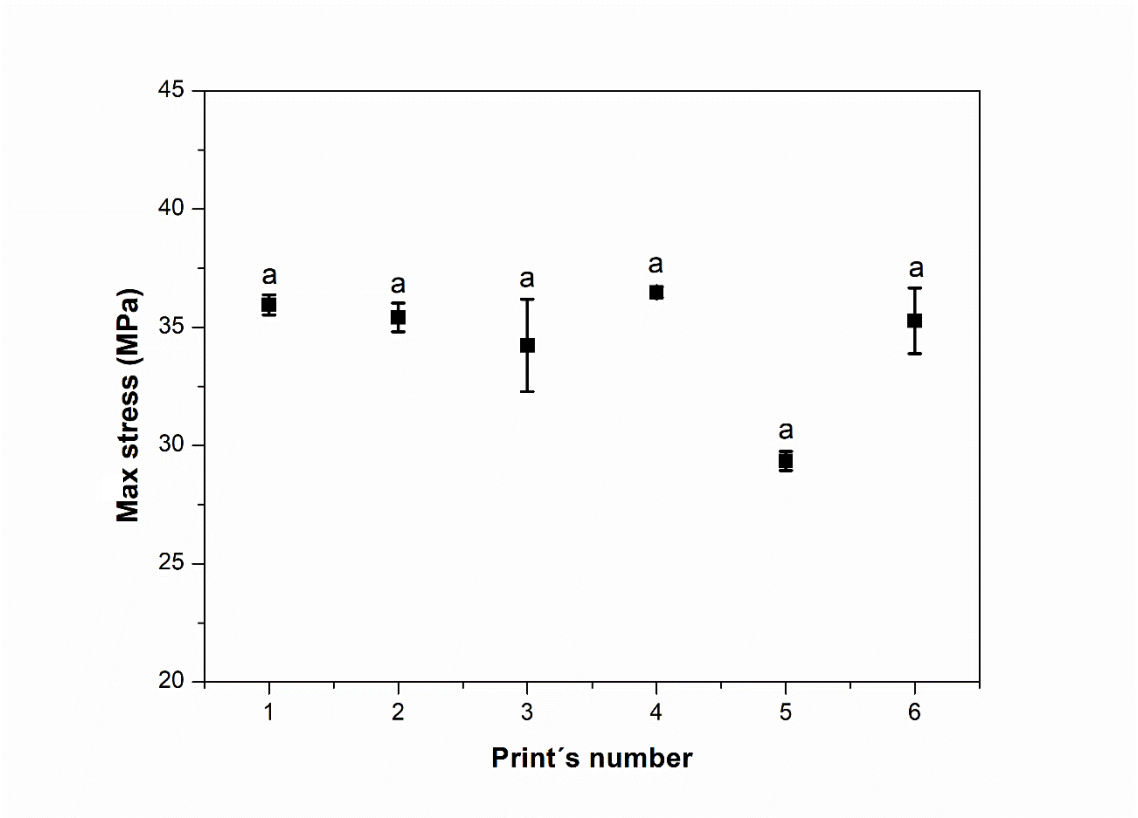

Figure 30 - Maximum stress reached for the horizontal TP.

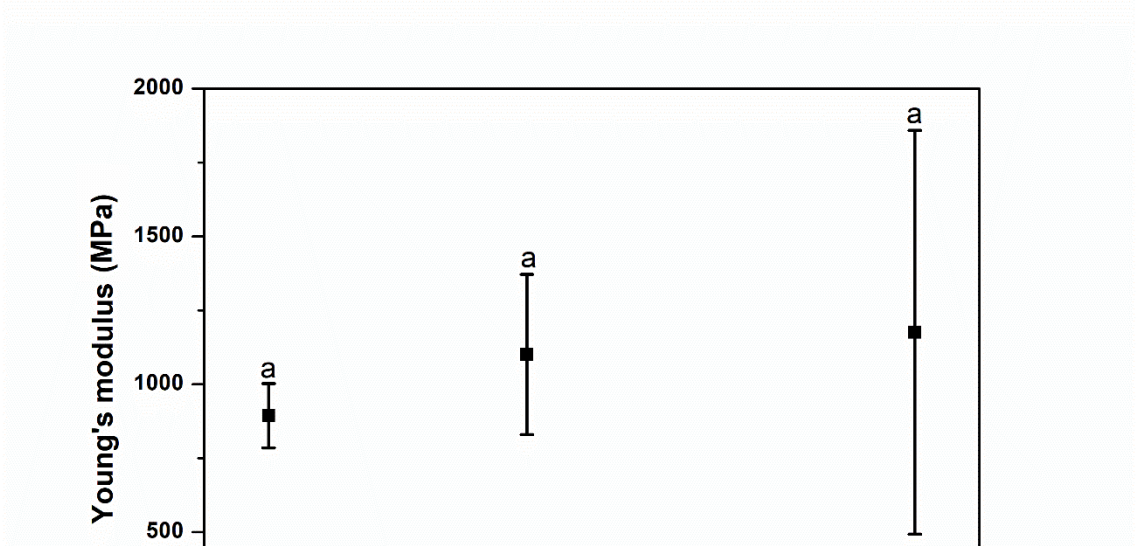

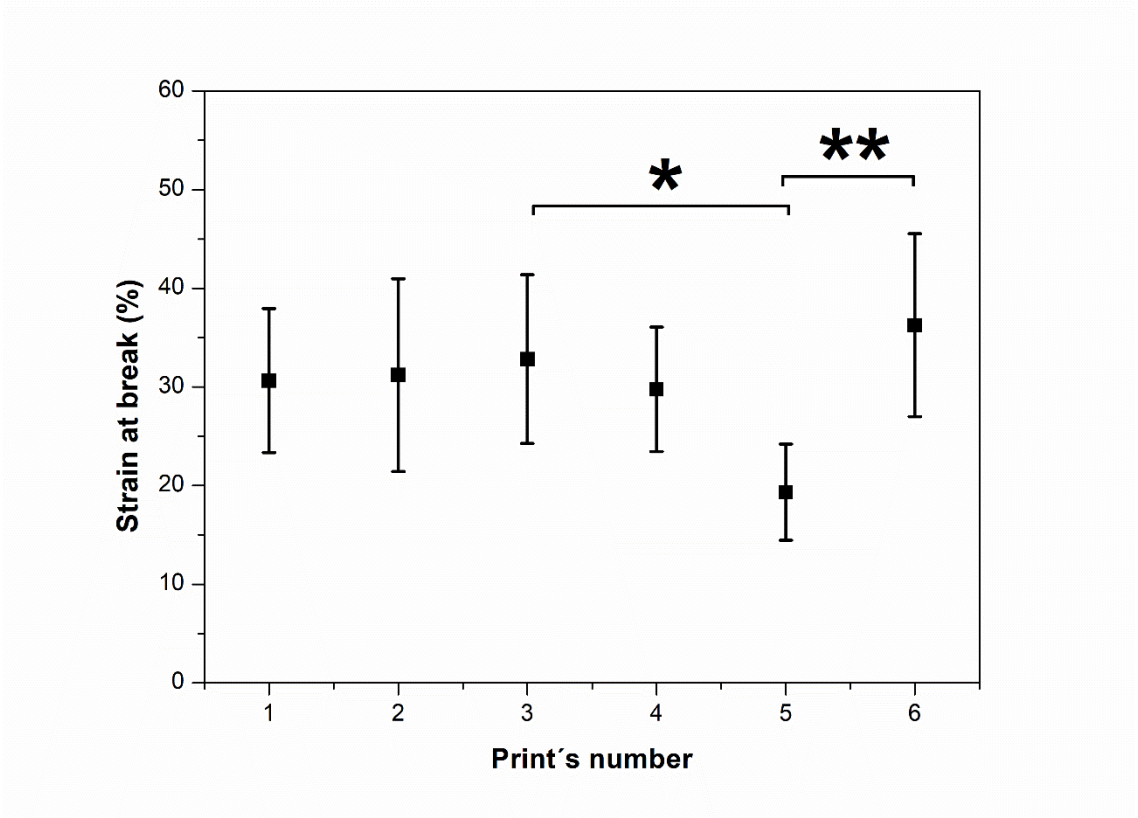

Figure 32 - Strain at break for the horizontal TP.

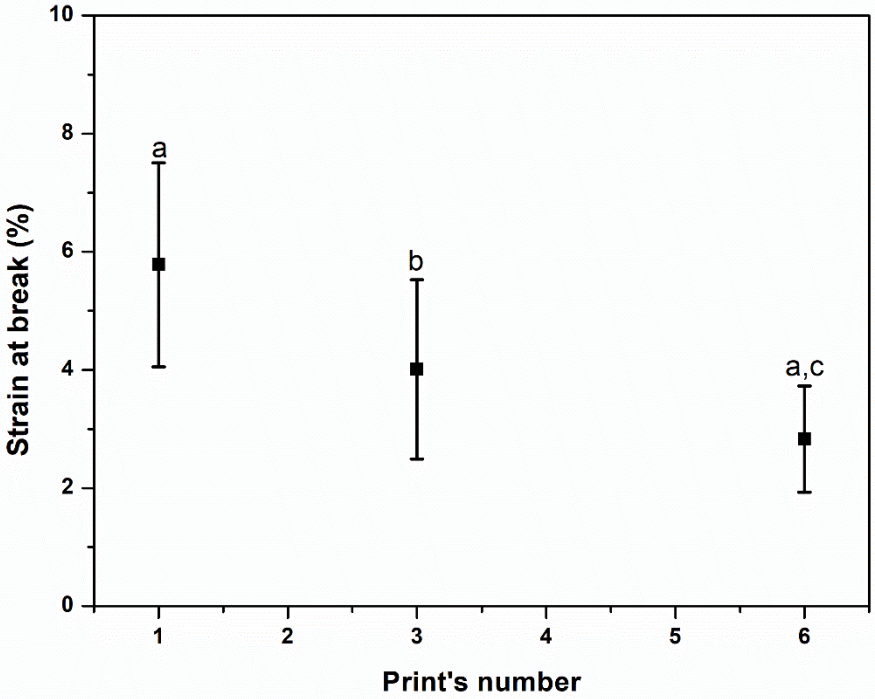

Figure 34 - Strain at break for the vertical TP.

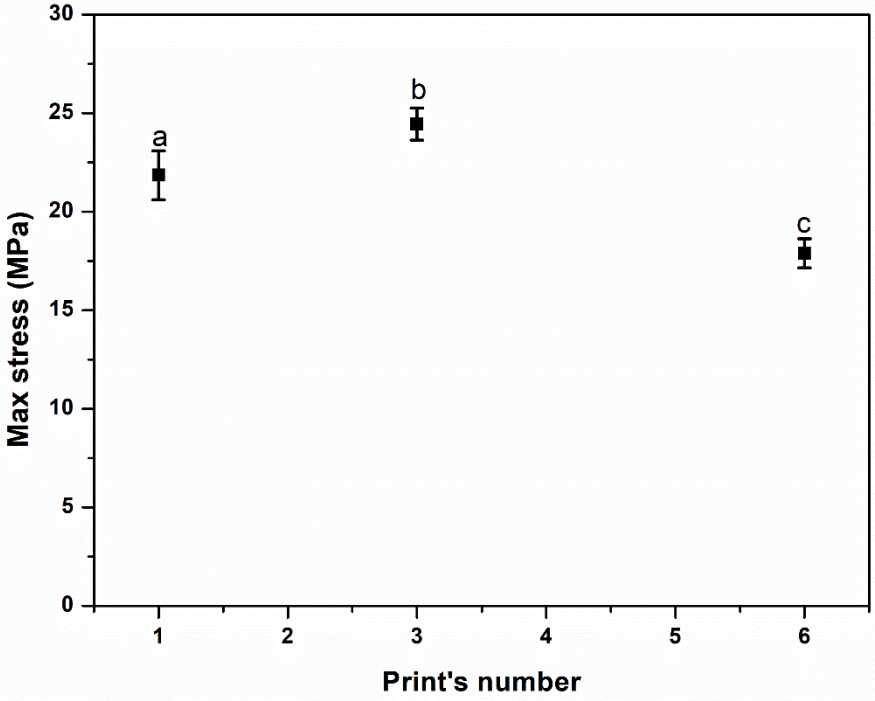

Figure 33 - Maximum stress reached for the vertical TP.

Table 7 - Summary of the results obtained in the mechanical characterization.

Cycle and orientation	Young Modulus (MPa)	Strai at break (%)	Máx stress (MPa)
1H	1178.14±138.31	30.63±7.30	35.95±0.43
2H	994.98±128.51	31.20±9.76	35.42±0.60
3H	1306.87±205.39	32.82±8.56	34.23±1.95
4H	1131.78±287.59	29.76±6.30	36.48±0.22
5H	1021.98±312.92	19.33±4.87	29.35±0.40
6H	1156.76±318.55	36.26±9.28	35.28±1.39
1V	894.22±108.84	5.78±1.73	21.86±1.24
3V	1101.00±270.6	4.01±1.52	24.45±0.81
6V	1175.97±683.09	2.83±0.90	17.90±0.74

4.2.2. Computed tomography

3D models like the one shown in Figure 35 were created for all analysed samples (which were all printed vertically to the printing table) and cross-section cuts (one cut of each print is presented in Figure 36 to Figure 38, were the zones highlighted in the samples are only informative for the software to calculate the porosity percentage presented in each one) were used for porosity analysis through its visualization in the software *Visual Graphics Studio*. The corresponding results are shown in Figure 41. Again, in this figure, statistically homogeneous groups are represented by the same letter. Lastly, longitudinal cuts were made in each sample to better visualize the shape of the samples, one of these cuts for each print is presents below in Figure 40.

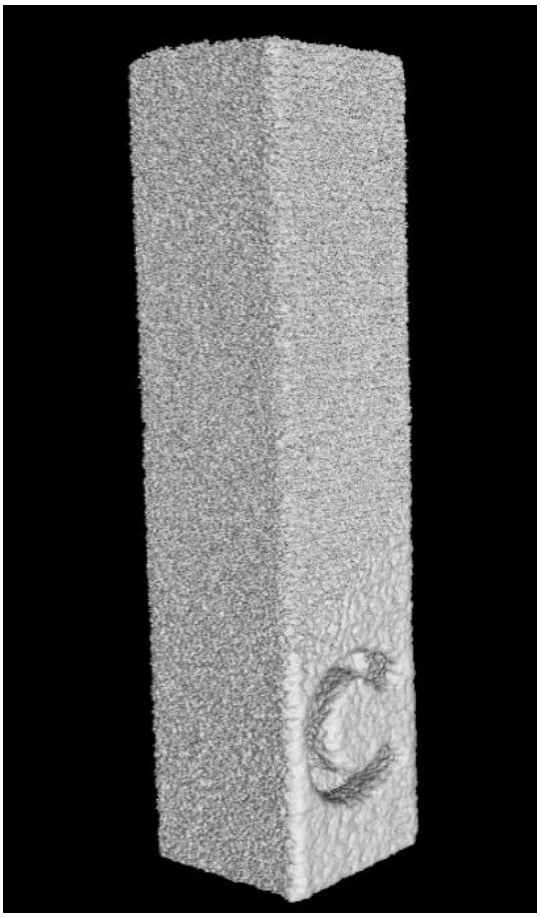

Figure 36 - Example of a 3D view, created in CT analysis of one of the samples analysed.

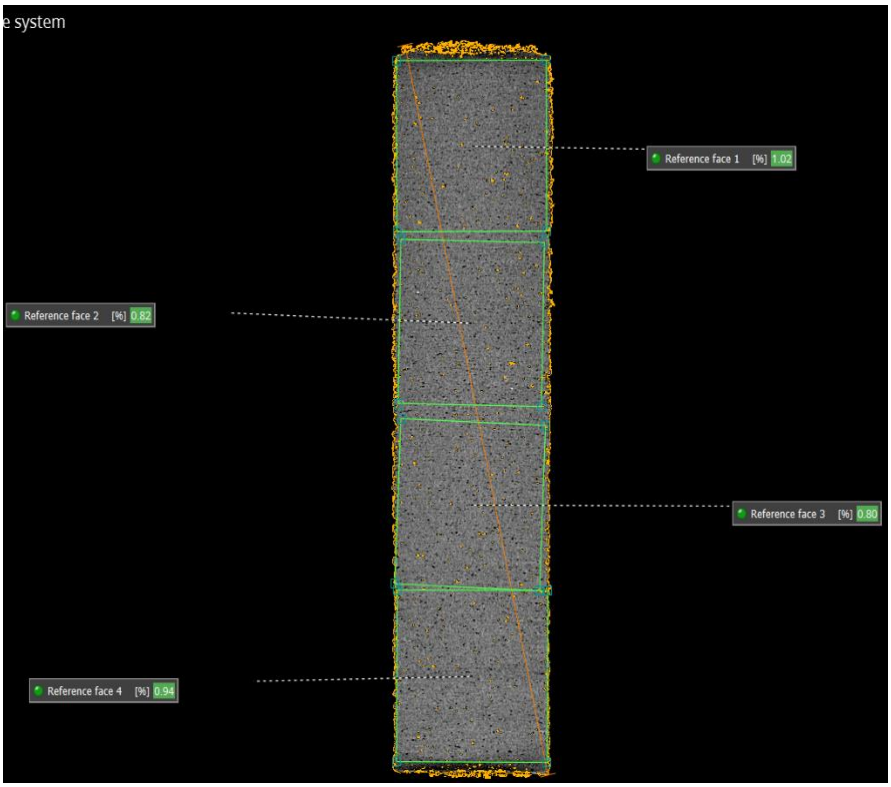

Figure 35 – Cross-section cut of the sample printed in the middle of the printing table from cycle 1.

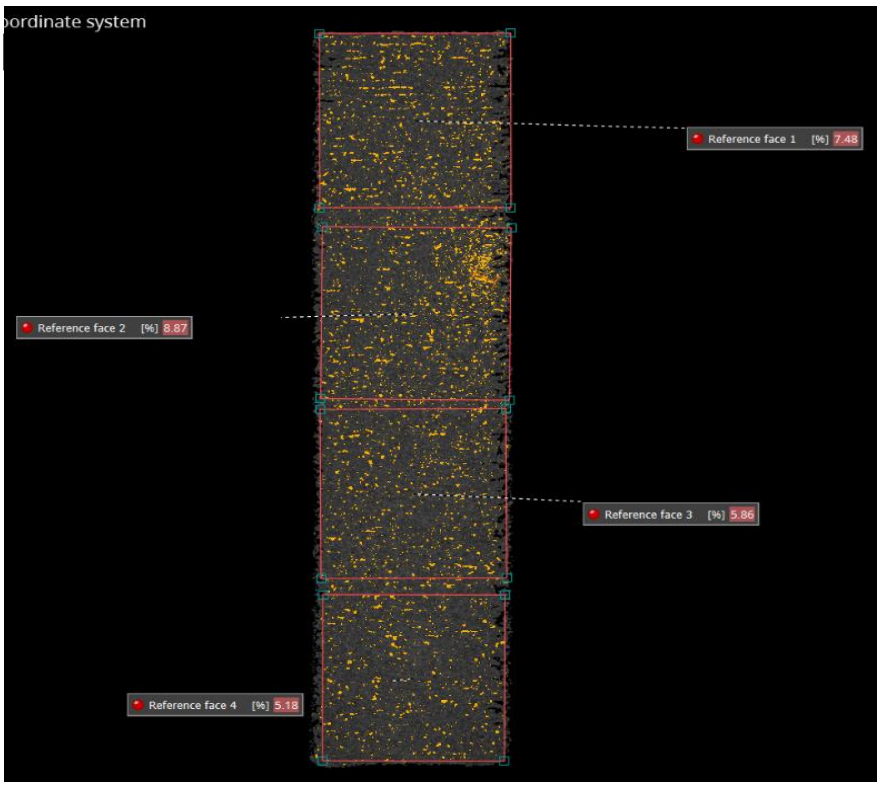

Figure 37 - Cross-section cut of the sample printed in the middle of the printing table from cycle 4.

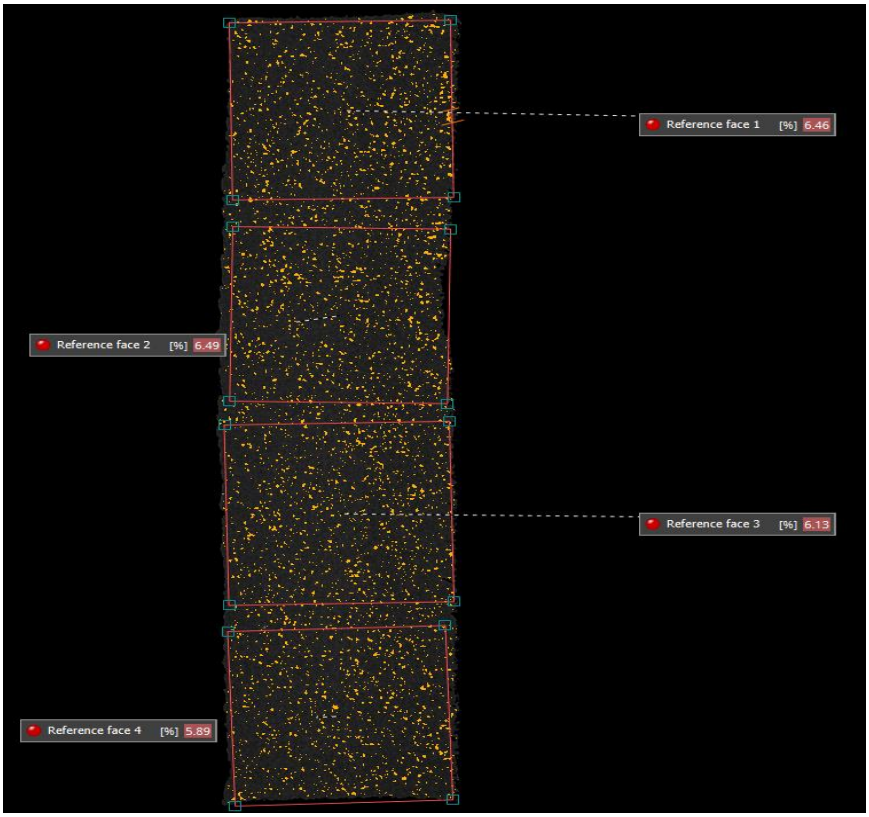

Figure 38 - Cross-section cut of the sample printed in the middle of the printing table from cycle 12.

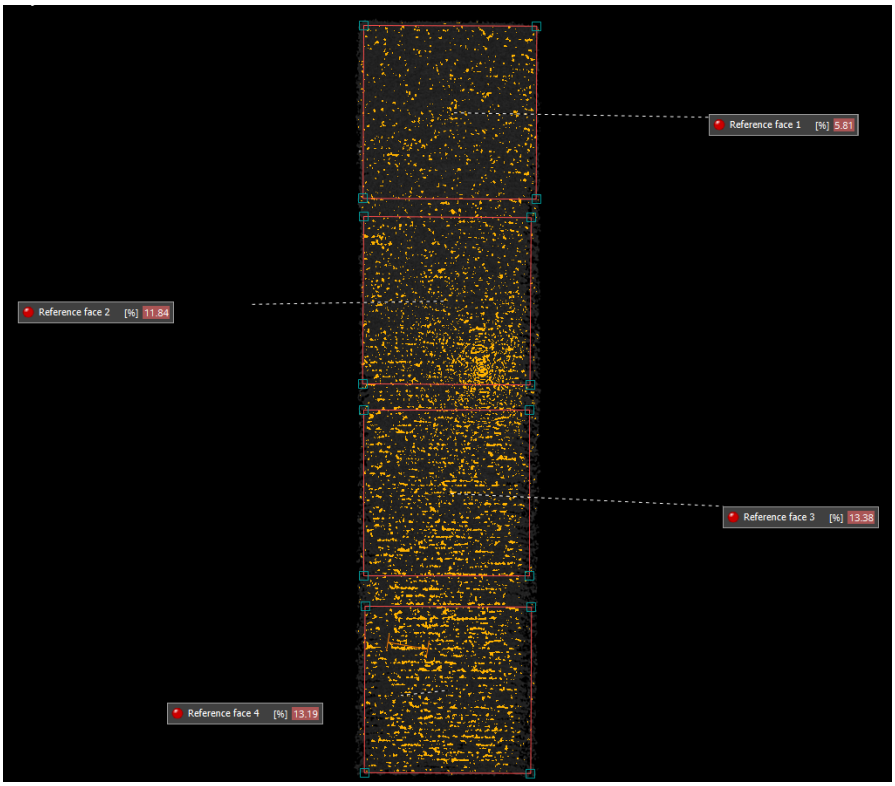

Figure 40 - Cross-section cut of the sample printed in the middle of the printing table from cycle 8.

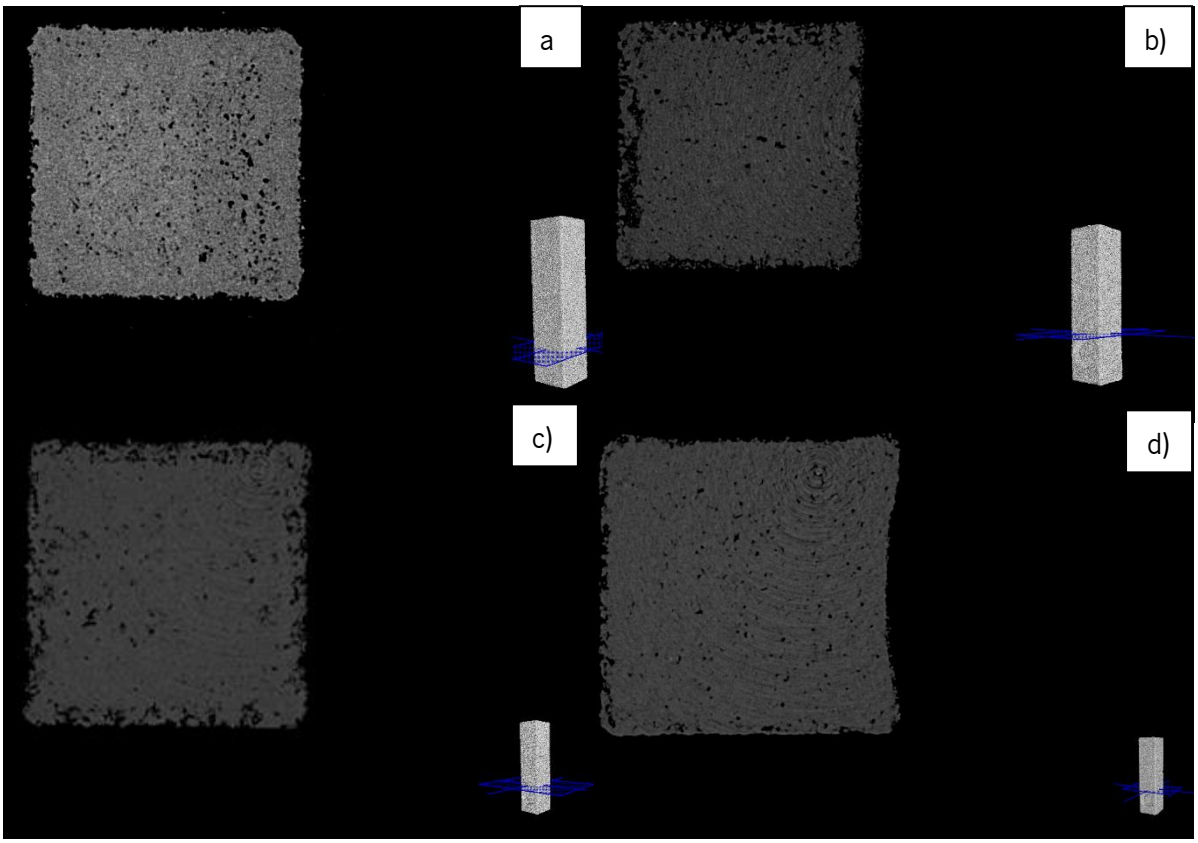

Figure 39 - Longitudinal cuts made for the center sample at 5mm from the base for; a) print 1; b) print 4; c) print 8; d) print 12.

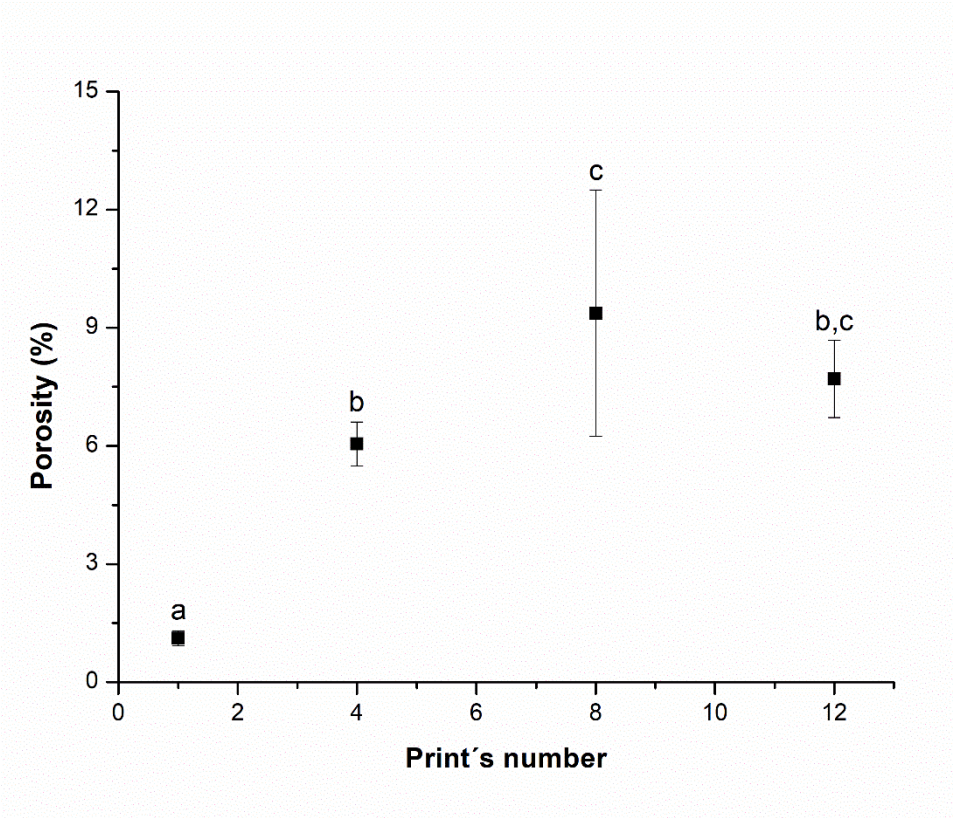

Figure 41 - Results obtained through CT analysis of the samples for cycles number 1, 4, 8 and 12.

Table 8 - Summary of mean porosity values obtained in the CT scan characterization.

Cycle	Mean porosity (%)	Standard deviation
1	1.11	0.19
4	6.05	0.56
8	9.37	3.13
12	7.7	0.98

Note: ANOVA and Tukey analysis, is represented by the letters and the asterisks in the graphics shown. When asterisk is shown, the groups have statistically significant differences between then. Also, when the letter differs between the groups, statistically significant differences are also apparent.

Note: in cycle 1, due to a machine error, the sample printed on the left side of the building table, was erased from the STL file and was not printed, only the right and center samples were, as such only those 2 samples were considered in the mean value calculated for porosity.

Through the analysis of 12 zones obtained from 3 different cross-section cuts made in each sample, it was noticeable that the mean porosity of the samples increases with the reprocessing cycles, with statistically significant differences between almost all the reprocessing cycles. This result might be related to the increased porosity observed in the powders as the printing cycles increased (Figure 27). It is also noticeable a decrease in porosity between printing cycles 8 and

12. However, as shown in Figure 40d) , there is a clear deformation in the samples of the 12th printing cycle. This deformation might be due to the collapse of the walls of the sample, which may fill the void left by extreme porosity. If this is the case, porosity will be artificially diminished.

4.3. Visual analysis

As the printing cycles increased, it was possible to notice some visual changes that happen in the printed parts due to the degradation of the powders. Figure 42 and Figure 43 show 2 parts printed alongside the samples for this thesis, one with 100% virgin powder and reused powders and other with 100% reused powders with 12 reprocessing cycles. As can be observed, the printed part with virgin powders presents a white and smooth surface, while the part printed with reused powders presented a yellowish color and much rougher surface. Another factor observed in the printed parts with reused powders is that thinner parts present a much lower resistance to bending than printed parts with virgin powders.

Figure 42 - Produced part with 100% virgin powder.

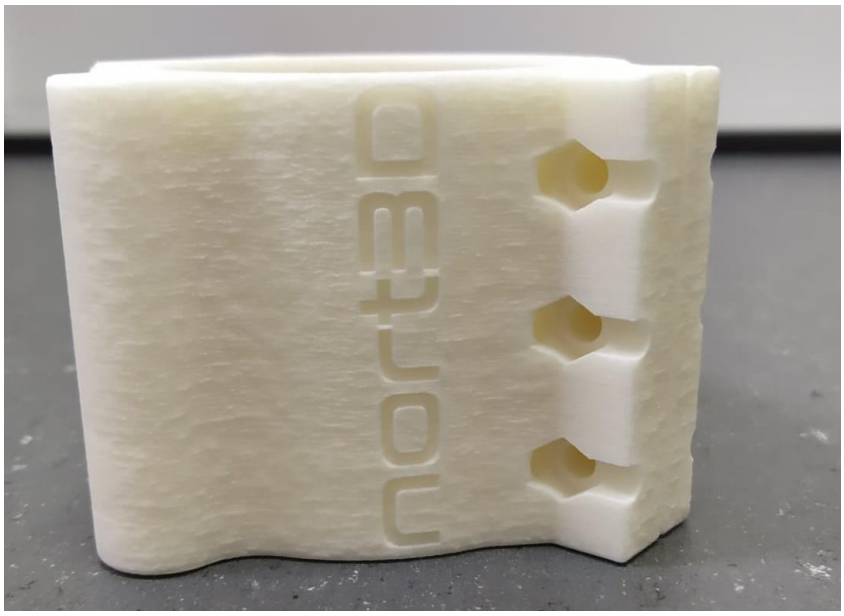

Figure 43 - Produced part with 100% reused powder with 12 reprocessing cycles.

4.4. Prediction method

Firstly, this technology is relatively unexplored, thus, there are still a lot of variables that might dictate the behavior that is not expected, and it might be different from the one observed in other production techniques such as injection moulding. One of the possible differences is the filtration process performed. Prior to the printing process, the filtration was thought to only destroy the bigger agglomerates that are formed during printing. However, it is clear that this step affects the whole process of the powders recycling process, not only in this way but also by excluding the worst powder from the equation, the reason why we believe that some properties characterised have shown slight to no difference between printing cycles.

The obtained mechanical properties showed only a slight decay (degradation) along the printing cycles tested. A degradation of the powders could be observed, but in a way not similar neither to injection molding, the process used by Bernardo et. al [27] to predict the decay of polymer properties, neither to the results of Lopes et. al [29]. Therefore, it is not possible to relate these characterizations with the prediction method developed by Bernardo and used by Lopes.

Chapter 5 – Conclusions and future works

5. Conclusions

SLS technology is a very versatile production process, although, as verified during the elaboration of this thesis, when 100% of the material used is reused from precious cycles, it does have difficulties in manufacture parts with reproducible properties. As demonstrated by all the characterizations performed through this thesis showed that this technique has some difficulties reproducing the same results not only in different printing cycles but also among the same cycle, even when the powders is relatively new.

With the limitations of this thesis, the following conclusions can be drawn:

The degradation of the powders with successive use is apparent. The DSC analysis showed a clear decrease in melting enthalpy (and melting temperature in the second heating) which means that the degree of crystallization is gradually decreasing throughout the reprocessing process. This might be an indication of chain scission, a phenomenon described in the literature. This leads to shorter chains that have higher mobility, which turns more difficult the crystallization process. Also, the fact that in the first heating the melting point does not vary, might indicate the contrary phenomenon in earlier stages of degradation, cross-linking, this creates ramifications on the chains, difficulting the melting process. In the SLS equipment, there is only one heating stage for the printing process so the melting temperature of the powders might not change throughout the cycles.

Moreover, the degradation of the powders was observed by SEM/EDS. Firstly, the surface of the powders after 12 printing cycles showed an increased porosity roughness when compared with the virgin powders. EDS showed an increase in the nitrogen detected in the 12th reprocessing cycle powders when compared to the virgin powders. This means that the material is reacting with the nitrogen used as a purge gas and incorporating it into its structure, affecting its appearance and behaviour.

The mechanical characterization showed that in terms of loss of properties, these only start to be significant in relatively high reprocessing cycles. Throughout the printing cycles the results showed that at least for these first cycles, mechanical properties might worsen slightly, but for the most part, tend to stay the same. Namely, the strain detected at break seems to be the most affected property. This aligns with the observed in the printed parts, especially with thinner ones when printed with reused powders, which tend to break easily. These tests, also show that the reliability

of the SLS technology only gets worse throughout the recycling process, failing to reproduce parts with the same mechanical performance even in the same batch, as demonstrated by the increase in the standard deviation of the properties analyzed. Also, this characterization showed that parts printed vertically have worse mechanical performance than those printed horizontally. As such it is easy to conclude that this printing orientation should be avoided when printing mechanically functional parts to prevent these to fail when in service, even if they are printed with virgin powder.

CT analysis shows what was expected when powders were observed in SEM. The higher the reprocessing cycle, the higher the porosity of the printed part. This can be so severe that for the 12th reprocessing cycle, it seems that a big void promoted the collapse of the external walls of the samples. This phenomenon is extremely negative for parts that have engineering applications since it could mean the premature failure of the part and/or a lack of dimensional accuracy.

The visualization of parts printed with new and reused powder, shows that smoother and clearer surfaces are nearly impossible to obtain with reused powder.

Lastly, as the objective was to reproduce the fabrication method used in *NM3D Ibérica,* their filtration system was used, and it proved to be a minimizer of material degradation. Considering the low loss of mechanical properties, it can be said that the filtration used acts in a way similar to the addiction of large quantities of virgin powder acted in the studied developed in [29].

In conclusion, degradation of the powders is apparent and unavoidable. This degradation might render the powders unusable especially in later reprocessing cycles. It compromises the correct behavior of printed parts and drastically fails in reproducing parts with the same performance (example: mechanical resistance, mean porosity, and melting temperature), as seen with the increase in the standard deviation through the cycles. Aa additional advantage of this process (besides the versatility that it offers) is that the filtration of the used powder helps to maintain its quality for longer.

5.1. Future works

Although this thesis showed the expected degradation of the powder used in the SLS printing process, further investigation is needed to better understand how it works, how it can be controlled, and also how can the powders be treated when they reach their end-of-life cycle.

Therefore, some suggestions may be considered for future works:

To study of mechanical properties in a larger range of reprocessing cycles, allowing a wider understanding. To study the degradation of the material without the filtration system being used and comparing it to when it is. To determine molecular mass of the polymer along the different reprocessing cycles, in order to better understand the degradation mechanisms involved. To development/adapt a mathematical method able to predict the evolution of properties along printing cycles. And finally, to study ways to reuse/recycle/treat the powders when the end of life is reached, as this is a important aspect that should be considered, as this technology has a large quantity of wasted material.

References

[1] Y. Zhai, D. A. Lados, and J. L. Lagoy, "Additive Manufacturing: Making imagination the major Limitation," *JOM*, vol. 66, no. 5, pp. 808–816, 2014.

[2] S. K. Tiwari, S. Pande, S. Agrawal, and S. M. Bobade, "Selection of selective laser sintering materials for different applications," *Rapid Prototyp. J.*, vol. 21, no. 6, pp. 630–648, 2015.

[3] Formlabs, "Guide to Selective Laser Sintering (SLS) 3D Printing," 2021. [Online]. Available: https://formlabs.com/blog/what-is-selective-laser-sintering/#What is Selective Laser Sintering 3D Printing%3F. [Accessed: 02-Mar-2021].

[4] R. D. Goodridge, R. J. M. Hague, and C. J. Tuck, "Effect of long-term ageing on the tensile properties of a polyamide 12 laser sintering material," *Polym. Test.*, vol. 29, no. 4, pp. 483–493, 2010.

[5] F. Kuehlein, D. Drummer, D. Rietzel, and A. Seefried, "Degradation Behaviour and Material Properties of PA12-Plastic Powders Processed by Powder Based Additive Manufacturing Technologies," in *3rd DAAAM-ICAT*, 2010, vol. 21, no. 1.

[6] D. T. Pham, S. Dimov, and F. Lacan, "Selective laser sintering: applications and technological capabilities," *Journel Eng. Technol. Capab.*, vol. 213, pp. 435–449, 1999.

[7] S. Kumar, "Selective Laser Sintering: A Qualitative and Objective Approach," *JOM*, vol. 55, no. 10, pp. 43–47, 2003.

[8] N. P. Karapathis, J.-P. S. van Griethuysen, and R. Glardon, "Direct rapid tooling: a review of current research," *Rapid Prototyp. J.*, vol. 4, no. 2, p. 13, 1998.

[9] J. P. Kruth, M. C. Leu, and T. Nakagawa, "Progress in additive manufacturing and rapid prototyping," *CIRP Ann. - Manuf. Technol.*, vol. 47, no. 2, pp. 525–540, 1998.

[10] R. Bogue, "3D printing: The dawn of a new era in manufacturing?," *Assem. Autom.*, vol. 33, no. 4, pp. 307–311, 2013.

[11] M. Attaran, "The rise of 3-D printing: The advantages of additive manufacturing over traditional manufacturing," *Bus. Horiz.*, vol. 60, no. 5, pp. 677–688, 2017.

[12] T. Wholers and T. Gornet, “History of Additive Manufacturing,” 2016.

[13] R. J. Wang, L. Wang, L. Zhao, and Z. Liu, “Influence of process parameters on part shrinkage in SLS,” *Int. J. Adv. Manuf. Technol.*, vol. 33, no. 5–6, pp. 498–504, 2007.

[14] K. Wudy, D. Drummer, F. Kühnlein, and M. Drexler, “Influence of degradation behavior of polyamide 12 powders in laser sintering process on produced parts,” *AIP Conf. Proc.*, vol. 1593, no. February, pp. 691–695, 2015.

[15] C. Mielicki, B. Gronhoff, and J. Wortberg, “Effects of laser sintering processing time and temperature on changes in polyamide 12 powder particle size, shape and distribution,” in *AIP Conference Proceedings*, 2014, vol. 1593, no. 1, January, pp. 728–731.

[16] J. Kruth, B. Vandenbroucke, J. Vaerenbergh, and P. Mercelis, “Benchmarking of different SLS/SLM processes as rapid manufacturing techniques,” *Int. Conf. Polymers & Moulds Innovations (PMI), Gent, Belgium, April 20-23*. pp. 1–7, 2005.

[17] E. D. Bain, “Polymer Powder Bed Fusion Additive Manufacturing: Recent Developments in Materials, Processes, and Applications,” *ACS Symp. Ser.*, vol. 1315, pp. 7–36, 2019.

[18] F. M. Mwania, M. Maringa, and K. van der Walt, “A Review of Methods Used to Reduce the Effects of High Temperature Associated with Polyamide 12 and Polypropylene Laser Sintering,” *Adv. Polym. Technol.*, pp. 1–11, 2020.

[19] S. Dadbakhsh, L. Verbelen, O. Verkinderen, D. Strobbe, P. Van Puyvelde, and J. P. Kruth, “Effect of PA12 powder reuse on coalescence behaviour and microstructure of SLS parts,” *Eur. Polym. J.*, vol. 92, no. 1, May, pp. 250–262, 2017.

[20] C. Hansen, “Materials Spotlight: The Properties of Nylon 12,” 2021. [Online]. Available: https://www.cableorganizer.com/learning-center/articles/materials-nylon12.html. [Accessed: 20-Mar-2021].

[21] L. Duddleston, “Polyamide (Nylon) 12 Degradation during the Selective Laser Sintering (SLS) Process : A Quantification for Recycling Optimization,” University of Wisconsin, 2015.

[22] G. Ehrenstein and S. Pongratz, *Resistance and Stability of Polymers*, 1st editio. Hanser Publications, 2013.

[23] A. Katta, “Analysis of PA6 powder aging during the Selective Laser Sintering process,” Aelen University, 2019.

[24] E. I. Valko and C. K. Chiklis, “Effects of thermal exposure on the physicochemical properties of polyamides,” *J. Appl. Polym. Sci.*, vol. 9, no. 8, pp. 2855–2877, 1965.

[25] K. Wudy and D. Drummer, “Aging effects of polyamide 12 in selective laser sintering: Molecular weight distribution and thermal properties,” *Addit. Manuf.*, vol. 25, no. 1, November, pp. 1–9, 2019.

[26] M. Tomanik, M. Zmudzińska, and M. Wojtków, “Mechanical and Structural Evaluation of the PA12 Desktop Selective Laser Sintering Printed Parts Regarding Printing Strategy,” *3D Print. Addit. Manuf.*, vol. 8, no. 4, pp. 271–279, 2021.

[27] C. A. Bernardo, A. M. Cunha, and M. J. Oliveira, “An algorithm for predicting the properties of products incorporating recycled polymers,” *Adv. Polym. Technol.*, vol. 15, no. 3, pp. 215–221, 1996.

[28] C. A. Bernardo, “Derivation and validation of models to predict the properties of mixtures of virgin and recycled polymers,” in *Frontiers in the science and technology of polymer recycling*, G. Akovali, C. Bernardo, J. Leidner, L. Utracki, and M. Xanthos, Eds. Springer-Science+Business Media, B.V., 1997, pp. 215–248.

[29] A. C. Lopes, Á. M. Sampaio, C. S. Silva, and A. J. Pontes, “Prediction of SLS parts properties using reprocessing powder,” *Rapid Prototyp. J.*, vol. 27, no. 3, pp. 496–506, 2021.

[30] J. D. Menczel, L. Judovits, R. B. Prime, H. E. Bair, M. Reading, and S. Swier, “Differential scanning calorimetry,” in *Thermal analysis of polymers*, vol. 31, no. 6, J. D. Menczel and R. B. Prime, Eds. John Wiley & Sons, Inc., 2014, p. Chapter 2.

[31] G. Paul, “A Practical Introduction to Differential Scanning Calorimetry,” in *Principles and Applications of Thermal Analysis*, 2008, pp. 1–263.

[32] W. Zhou, R. Apkarian, Z. L. Wang, and D. Joy, “Fundamentals of scanning electron microscopy (SEM),” in *Scanning Microscopy for Nanotechnology: Techniques and Applications*, 2007, pp. 1–40.

[33] K. D. Vernon-Parry, “Scanning Electron Microscopy : An introduction,” *III-Vs Rev.*, vol. 13, no. 4, pp. 40–44, 2000.

[34] J. Goldstein, D. Newbury, D. Joy, C. Lyman, P. Echlin, and E. Lifshin, “The SEM and Its Modes,” in *Scanning Electron Microscopy and X-ray Microanalysis: Third Edition*, 2003, pp. 21–60.

[35] S. Nasrazadani and S. Hassani, “Modern analytical techniques in failure analysis of aerospace, chemical, and oil and gas industries,” in *Handbook of Materials Failure Analysis with Case Studies from the Oil and Gas Industry*, Texas, USA: Elsevier Ltd., 2016, pp. 39–54.

[36] H. Villarraga-Gómez, “Studies of Dimensional Metrology with X-Ray CAT Scan,” University of North Carolina at Charlote, 2018.

[37] H. University of Berlin, “Investigation of Polymers with Differential Scanning Calorimetry,” *Advanced Lab: DSC Investigation of Polymers*. Berlin, pp. 1–17, 2009.

[38] J. Vohlídal, “Polymer degradation: a short review,” *Chem. Teach. Int.*, vol. 1, p. 8, 2020.

[39] A. Kulkarni and H. Dasari, “Current Status of Methods Used in Degradation of Polymers: A Review,” in *MATEC Web of Conferences*, 2018, vol. 144, pp. 1–11.

ANNEX

Annex I – PA12 L1600 data-sheet

ProMaker **P SERIES** compatible powders **2019**

Laser sintering materials have been developed by Prodways and our partners to work in combination with ProMaker printers, offering an effective additive manufacturing solution for many applications, including functional prototyping and industrial needs.

	TPU-70 A[1]	PP 1200 [1]	PA12-L 1600 [1][3]	PA12-S 1550 [1]	PA12-GFX 2550 [1]
Specification	· Elastomeric material with 70 shore A · Elongation at break > 300% · No need for infiltration · Possibility to adjust shore based on energy input · High resolution	· Bringing the Polypropylene mechanical characteristics to the SLS® market, allowing the development of new applications · Easy to process and with a 30% Refresh rate	· General purpose material with excellent mechanical properties and high elongation at break · Low water absorption and easy to process · Good recyclability	· Fine granulometry for excellent outline and surface quality · Low porosity, UV stable · High recyclability for lower operating costs	· Glass beads & aluminium filled nylon for reinforced strength · Excellent behavior in temperature and good chemical resistance · Similar to PP20% injected parts · Low and homogeneous shrinkage · High recyclability for lower operating costs
Typical Application Examples	Prototypes and final parts for elastic structures, hoses, grips, bellows, bumpers, gaskets and seals, tubes, toys and modeling for Footwear, Automotive, Aerospace and Luxury	Parts that need ductility, Living hinges, Low friction elements, Chemical resistant needs, Low density parts (lighter)	Wide range of prototyping and rapid manufacturing applications	Prototyping and small series for a wide range of applications including Formula 1, Automotive, Medical, Aerospace, Military, Luxury industry	Mechanical parts in engine resisting temperature, parts for pumps, complex end-use parts with improved strength properties for a wide range of applications.
Appearance	White Glow in the dark Green/Blue	White/translucent	White	Natural + mass coloring Black/Blue/Red/Grey	Grey
Average particle size	62 µm	70 µm	N.A	42 µm	46 µm
Bulk Density	1.2 g/cm3	0.33 g/cm3	0.48 g/cm3	0.50 g/cm^3	1.05 g/cm3
Density of parts	1.12 g/cm3	0.89 g/cm3	0.95 g/cm3	0.98 g/cm3	1.35 g/cm3
Moisture absorption	N.A	N.A	N.A	0.50% (ASTM D570)	0.33% (ASTM D570)
Melting Point	105 °C to 122°C	136°C	183°C	181°C - 183 °C	181°C - 183 °C
Heat Deflection 1.8 MPa	N.A	53°C	83.5°C	86°C	116°C
Tensile Strength	7 MPa	28 MPa	46 MPa	44 MPa	30 MPa
Tensile Modulus	65 MPa	1250 MPa	1602 MPa	1550 MPa	2550 MPa
Elongation @ break	350%	25%	36%	15%	8%
Flexural Strength	21%	/	46.3 MPa	N.A	N.A
Flexural Modulus	N.A	1150 MPa	1300 MPa	1350 MPa	2275 MPa
Impact Strength (unnotched Izod)	No break	25 KJ/m^2	13.2 KJ/m^2	68 KJ/m^2	80 KJ/m^2
Shore Test	70 Shore A	72 Shore D	N.A.	68 Shore D	77 Shore D
Resistivity domain	Insulator	/	Insulator	Insulator	Antistatic
Upper facing processed & blasting, Surface Ra	N.A	/	N.A	7 µm	8 µm
Upper facing after Finishing, Surface Ra	N.A	/	N.A	7 µm	1 µm
Testing standard / Certification	ISO	ISO	GB/T	ISO	ISO
By	Prodways Materials	Prodways Materials	Prodways Materials by Farsoon	Prodways Materials	Prodways Materials

Annex II – Promaker P1000 data-sheet

ProMaker P1000 SPECIFICATIONS

	ProMaker P1000
Max. Build envelope size (LxWxH)	300 x 300 x 300 mm (11 x 11 x 11 in)
Volume Build Rate (max) * @0.10 mm layer thickness	0.9 l/hr 54 in³/h
Volume Build Rate (max) * @0.12 mm layer thickness	1.1 l/hr 67 in³/h
Scanning Speed	3.5 m/s (118 in/s)
Scan Spacing	0.15 - 0.30 mm 0.006 - 0.012 in
Layer thickness (typical)	0.06-0.12 mm (0.1 mm) 0.002-0.004 in (0.004 in)
Laser Type	30W CO_2
Laser beam size	450 µm
Laser Window	Removable, Easy to clean
Precision optics	F-theta-lens
Powder Feed Mode	Bi-directional powder feed system with two feed cylinders
Powder Delivery	Precision counter-rotating roller
Max. Chamber Temperature	200°C 392°F
Thermal Field Control	Ten independent heaters with four IR sensor & intelligent temperature control systems
Key Software Features	Slicing on the fly
Printer size (LxWxH)	1640 x 1000 x 1920 mm (65 x 39 x 76 in)
Weight	700 kg (1544 lb)
Data File Format	.STL / 3MF

* material, geometry and nesting density dependant